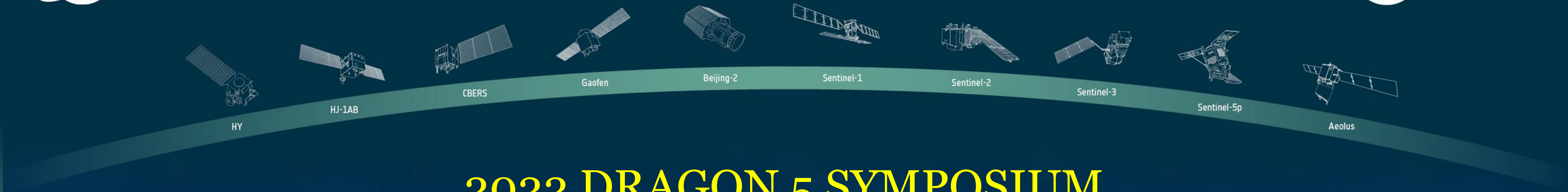

2022 DRAGON 5 SYMPOSIUM

MID-TERM RESULTS REPORTING

17-21 OCTOBER 2022

[PROJECT ID. 59257]

[MAPPING FOREST PARAMETERS AND FOREST DAMAGE FOR SUSTAINABLE FOREST MANAGEMENT FROM DATA FUSION OF SATELLITE DATA]

Dragon 5 Mid-term Results Project

<20/OCT/2022, 8:30AM - 10:00AM CEST>

ID. 59257

PROJECT TITLE: MAPPING FOREST PARAMETERS AND FOREST DAMAGE FOR SUSTAINABLE FOREST MANAGEMENT FROM DATA FUSION OF SATELLITE DATA

PRINCIPAL INVESTIGATORS: Prof. Xiaoli Zhang and Dr. Johan Fransson

CO-AUTHORS: Langning Huo, Ning Zhang, Henrik Persson, Yueting Wang, Eva Lindberg, Niwen Li, Ivan Huuva, Guoqi Chai, Lingting Lei, Long Chen, Xiang Jia, Zongqi Yao

PRESENTED BY: Xiaoli Zhang

Beijing Forestry University

Swedish University of Agricultural Sciences

Project Introduction

Background:

- This project concerns the topic Ecosystems and spans the subtopics Collaborative estimation of forest quality parameters and Forest and grassland disaster monitoring.

Objective:

- Study and explore remote sensing techniques in forest applications, especially on data fusion of satellite images, laser scanning, and hyperspectral drone images.

The research contents:

- Tree species classification
- Forest parameter estimation
- Forest insect damage detection

EO Data Delivery

ESA Third Party Missions	No. Scenes
1. Sentinel-1	133
2. Sentinel-2	330
3. SPOT	2
4.	
5.	
6.	
Total:	465

Study areas:
- Gaofeng, Yantai, Fushun, Lu'an, Wangyedian, Genhe and Pu'er in China
- Remningstorp in Sweden

Chinese EO data	No. Scenes
1. Gaofen-1	55
2. Gaofen-2	110
3. Gaofen-6	130
4.	
5.	
6.	
Total:	295

Study areas:
- Gaofeng, Yantai, Fushun, Lu'an, Wangyedian, Genhe and Pu'er in China

EO Data Delivery

The satellite images acquired for the study areas in China are:

- Sentinel-1, time-series images from 2019 to 2021, covering Gaofeng and Wangyedian.
- Sentinel-2, time-series cloud-free images from 2019 to 2021, covering Gaofeng, Lu'an, Wangyedian, Genhe, and Pu'er.
- Gaofen-1/2/6, 295 images from 2021 to 2022, covering Gaofen, Genhe and Pu’er.
- Radarsat-2, one image covering Fushun and one image covering Qingyuan.

The satellite images acquired in Remningstorp, Sweden are:

- Sentinel-2, time-series cloud-free images from 2018 to 2021.
- WorldView-3, one SWIR image (June 2021).
- Radarsat-2, one image each in 2020 and 2021.
- Pleiades, one image (29 Apr 2021).

Field Data Collection

- Field investigation of forest parameters was conducted in **Gaofeng, China**. The inventory recorded diameter at breast height, tree height, under branch height, and the coordinates of the plots.
- Spectral information was collected from healthy and pine nematode-infested forests at different stages in the **Fushun and Lu'an** study areas.

- The forest information of the sample plots in **Remningstorp** was updated. A controlled experiment was conducted for bark beetle infestation, and the infestation symptoms were recorded.

Tree Species Classification by few-shot learning (Stand scale)

- propose an improved prototypical networks (**IPrNet**) , a **CBAM-P-Net** model of the prototype network combined with an attention mechanism, and a **Proto-MaxUp+CBAM-P-Net** model of the CBAM-P-Net combined with a data enhancement strategy
- use UAVs hyperspectral data
- obtain good classification results for **8 major tree species** in southern China

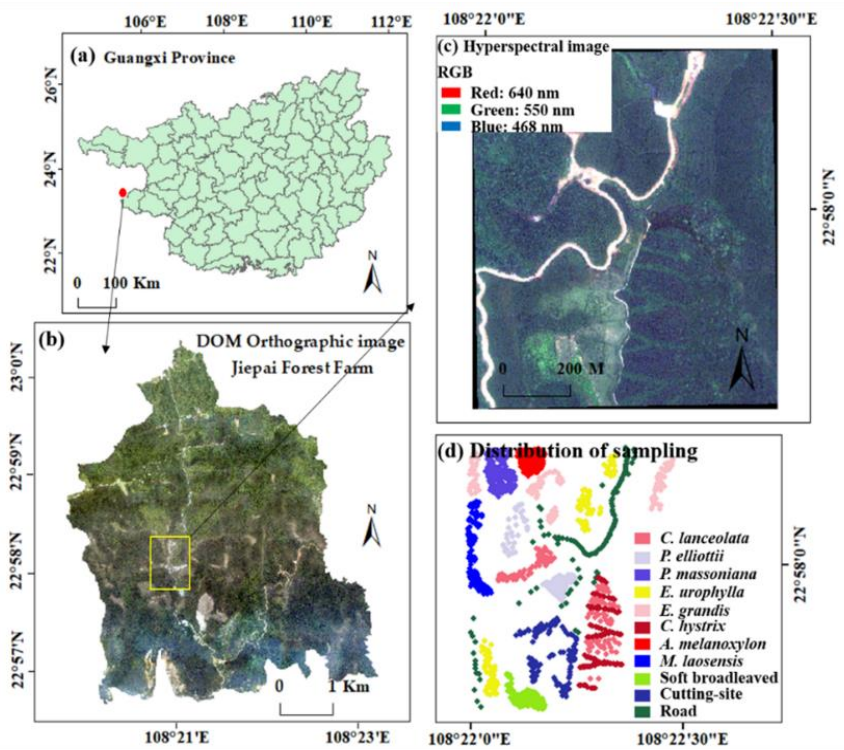

Categories	Samples	
	Trian	Test
Cunninghamia lanceolata	96	24
Pinus massoniana	96	24
Pinus elliottii	96	24
Eucalyptus grandis	96	24
Eucalyptus urophylla	96	24
Castanopsis hystrix.	96	24
Mytilaria laosensis	96	24
Acacia melanoxylon	96	24
Other broadleaf forest	96	24
Road	96	24
Cutting-site	96	24
Total	**1056**	**264**

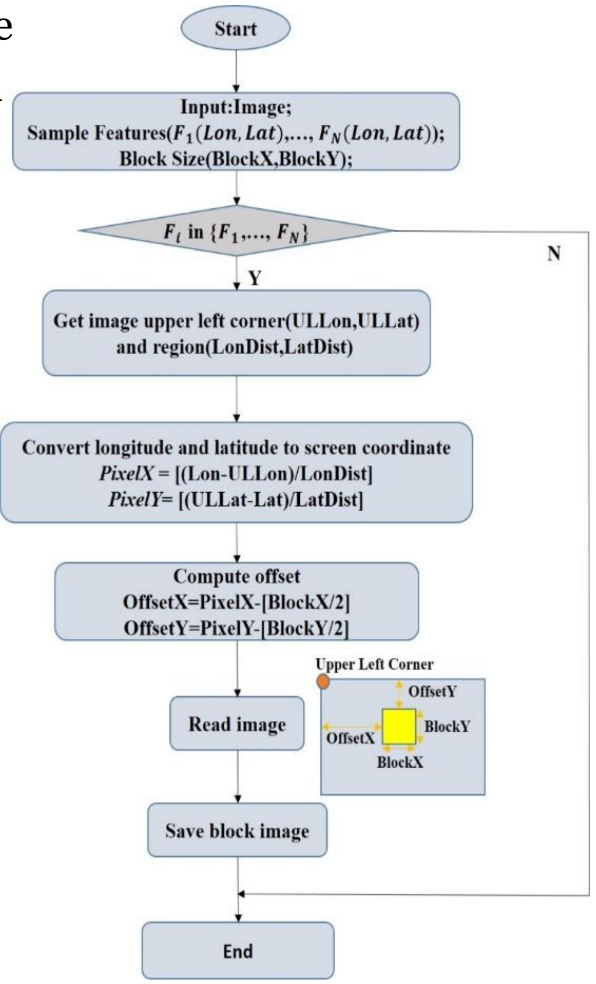

IPrNet Classification Framework

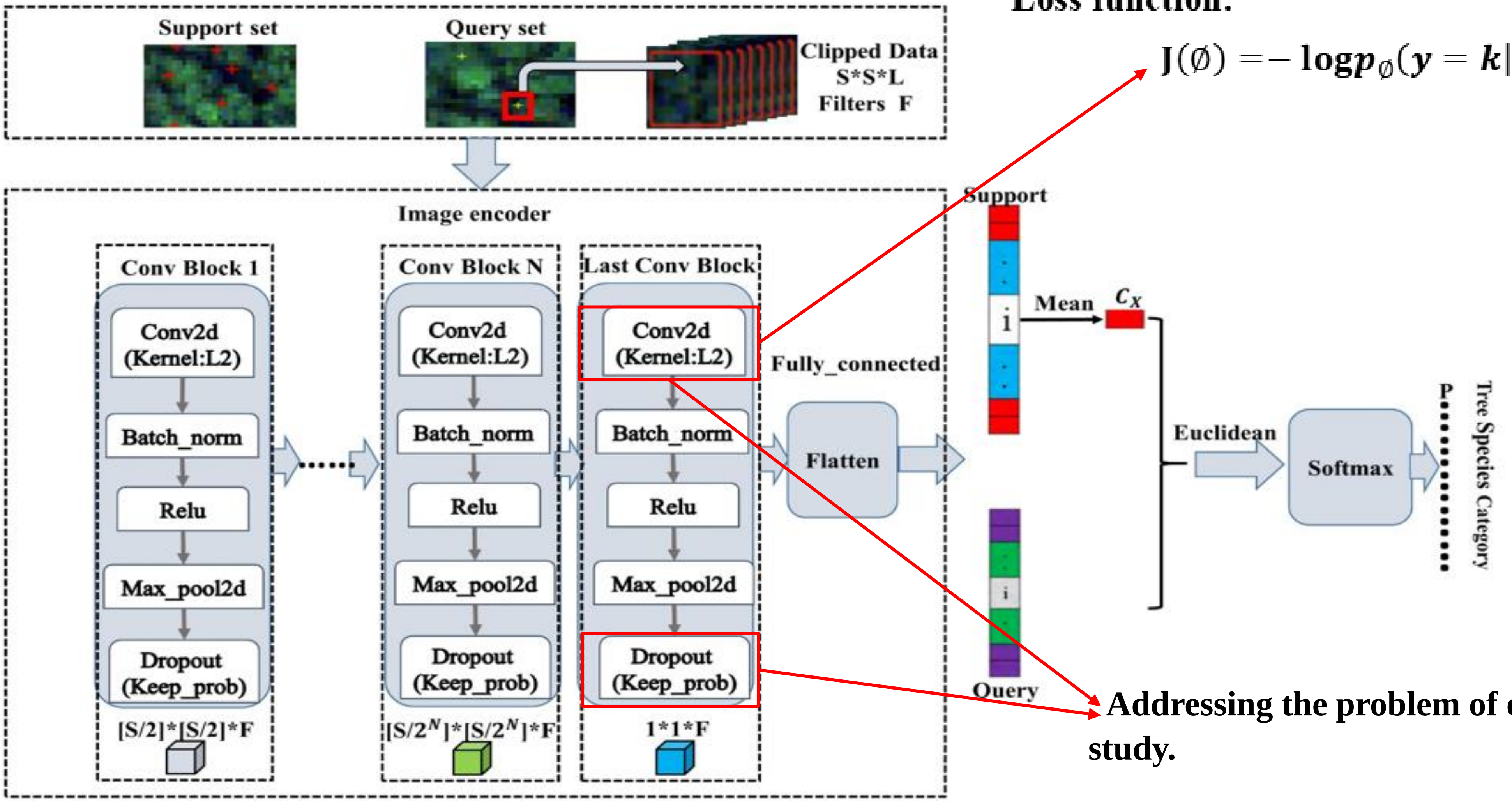

Loss function:

$$J(\emptyset) = -\log p_{\emptyset}(y = k|x) + \alpha_2 \sum_{w} w^2$$

Addressing the problem of overfitting in this study.

CBAM-P-Net Classification Framework

Target:

Improving the feature extraction efficiency
Overcoming the dimensional dilemma

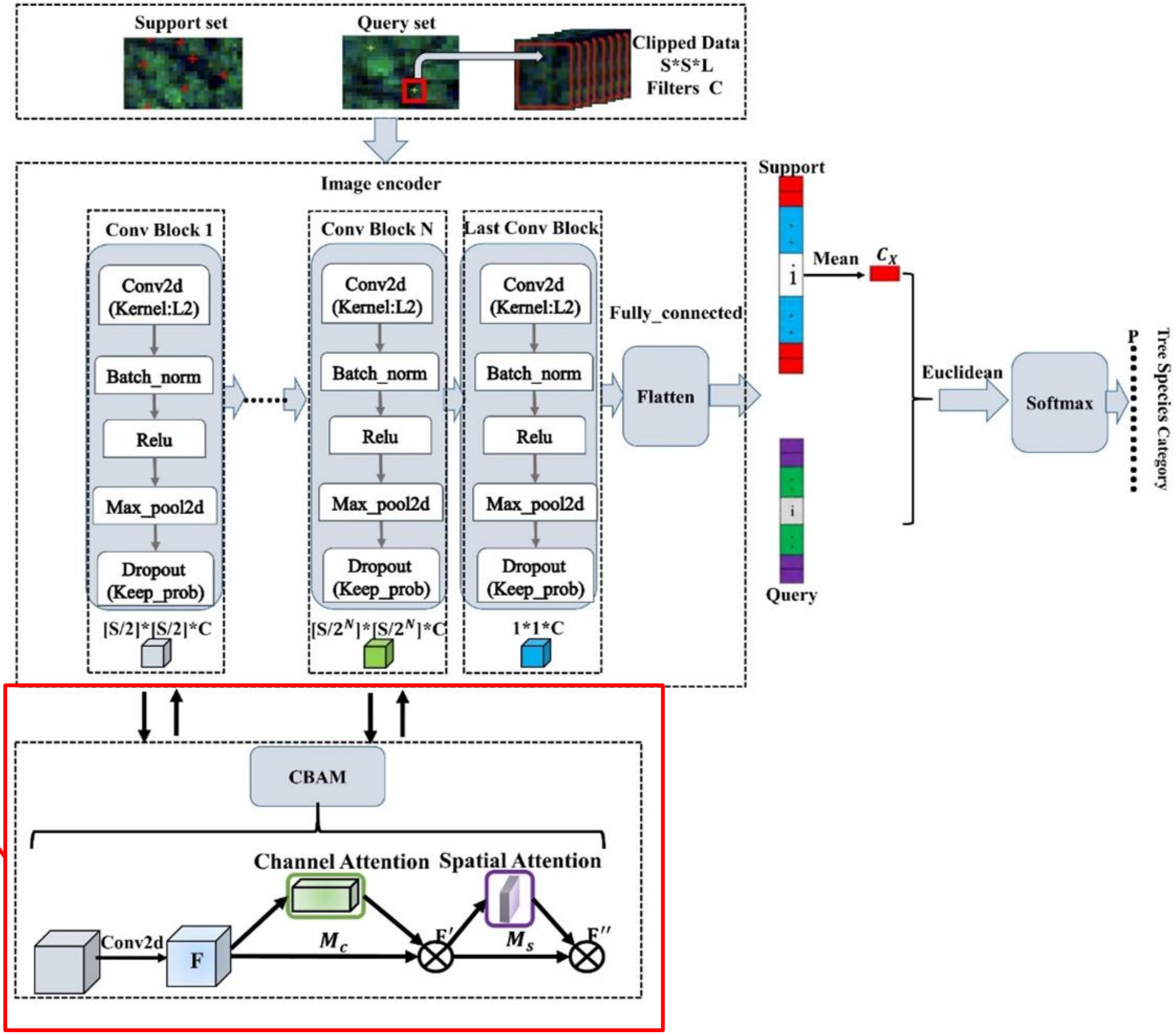

CBAM Combination Strategy:

- **Channel attention is applied globally**
- **Spatial attention is applied locally**
- **Channel First → Global first and then local**

Tree Species Classification

Proto-MaxUp Classification Framework

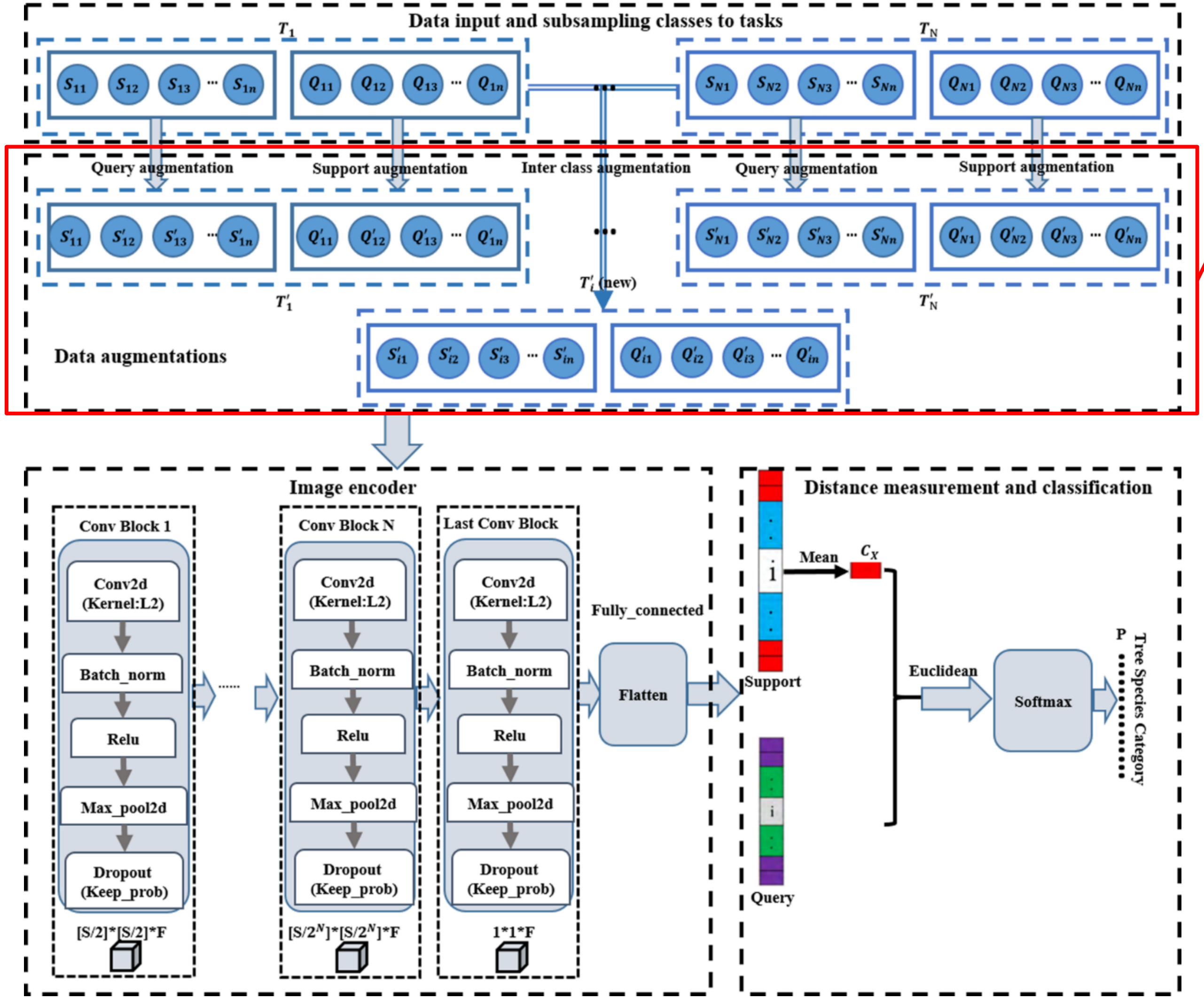

Data augmentation:
- Improving sample diversity.
- Minimizing the overfitting problem.

Proto-MaxUp:
- Adversarial training: minimize the maximum loss
- Solving the issue of saddle-point

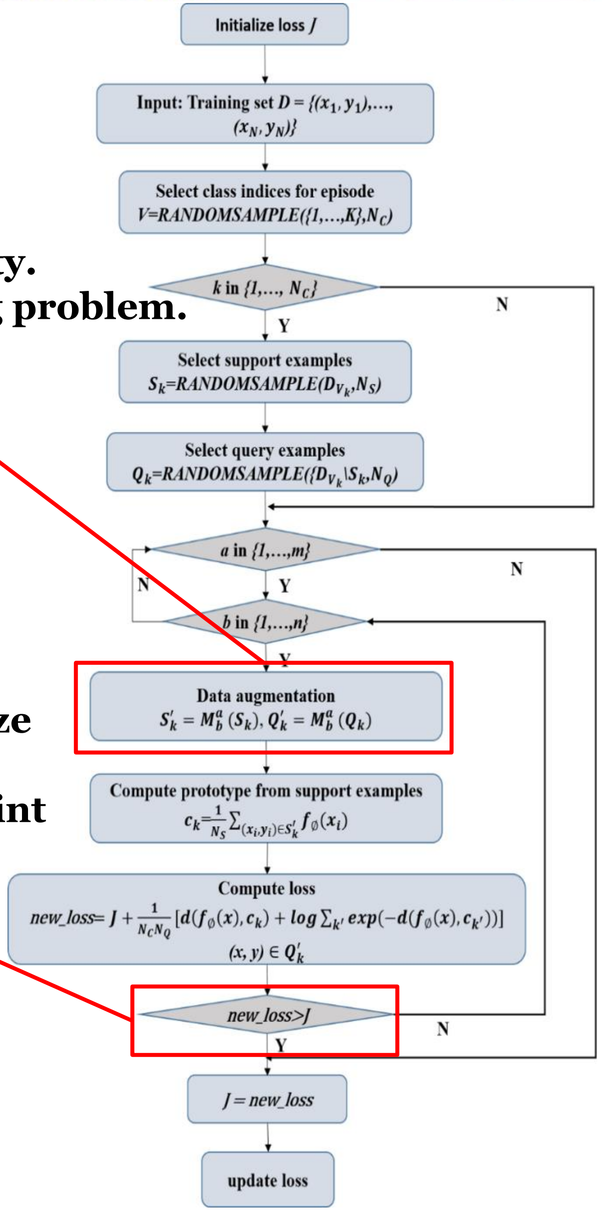

Tree Species Classification

IPrNet Classification Map

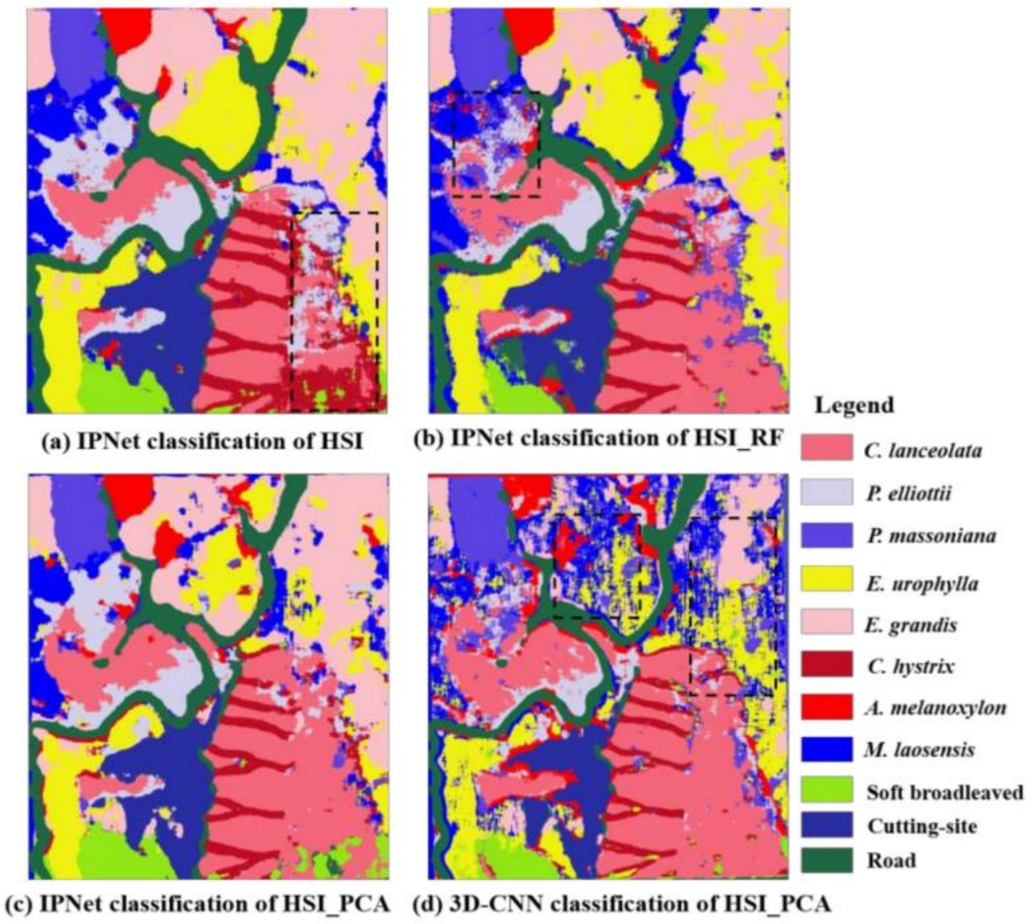

	27×27		
	OI	**RF**	**PCA**
Epochs/iterations	20/100	20/100	20/100
LEA	98.8%	98.86%	98.74%
OA	71.08%	94.49%	98.53%
Kappa	0.6819	0.9394	0.9838
Training Times (S)	2406	1308	1290
C. lanceolata	45.36%	91.86%	100%
P. elliottii	55.58%	78.62%	93.74%
P. massoniana	88.12%	99.62%	100%
E. urophylla	46.04%	87.82%	100%
E. grandis	55.74%	95.24%	100%
C. hystrix	93.14%	93.3%	98.18%
A. melanoxylon	73.38%	99.98%	99.92%
M. laosensis	49.36%	88.7%	99.5%
Soft broadleaved	83.76%	99.48%	96.02%
cutting-site	96.1%	100%	100%
Road	95.32%	100%	100%

Tian, X; Chen, L; Zhang, X *; Chen, E. Improved Prototypical Network Model for Forest Species Classification in Complex Stand. *Remote Sensing*, **2020,**12, 3839

CBAM-P-Net Classification Map

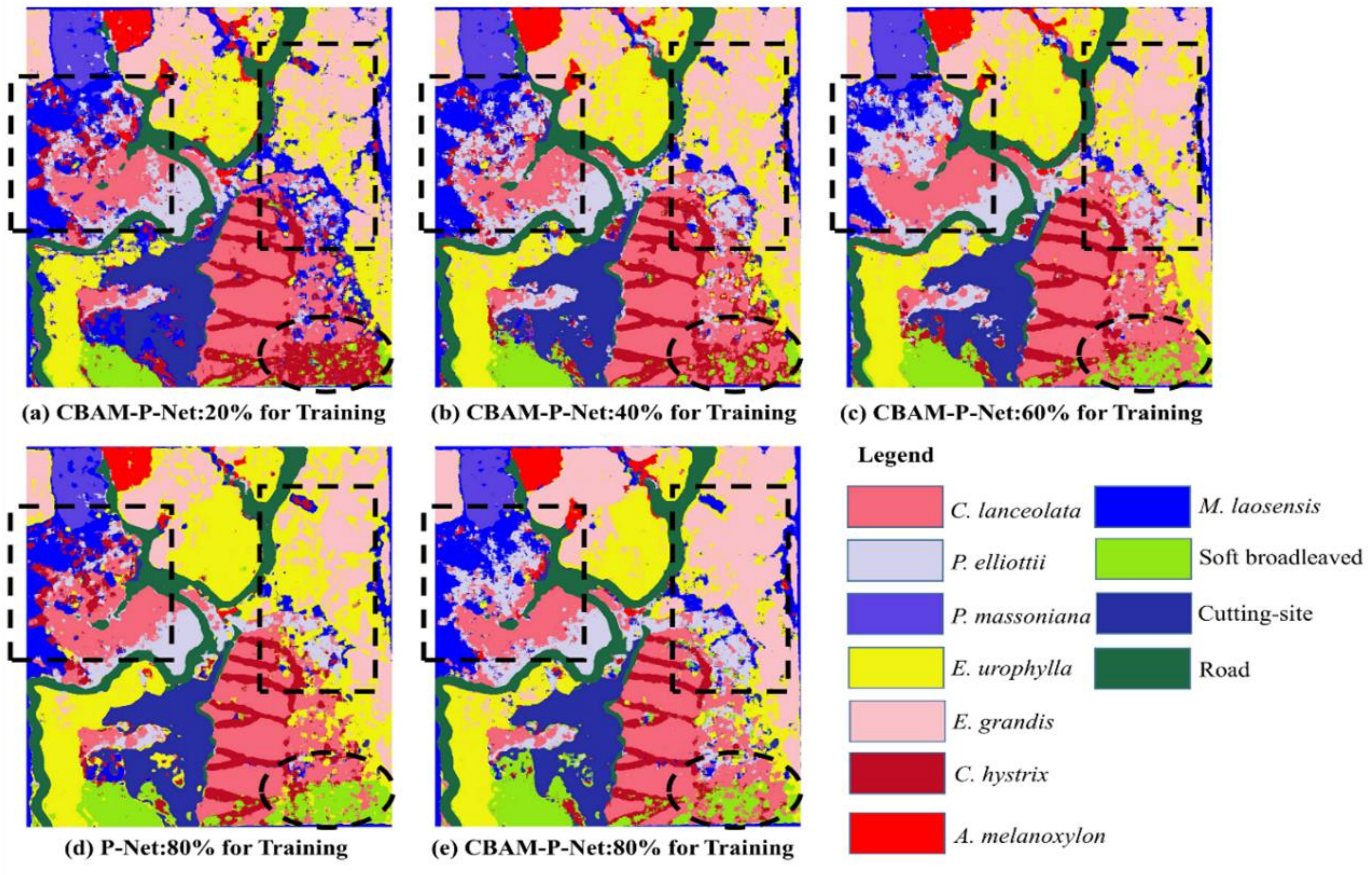

	17×17
Epochs/iterations	15/100
LEA	100%
OA	**97.28%**
Kappa	0.9701
Training Times (S)	1209
C. lanceolata	93.34%
P. elliottii	91.3%
P. massoniana	97.08%
E. urophylla	96.9%
E. grandis	99.74%
C. hystrix	92%
A. melanoxylon	99.96%
M. laosensis	99.92%
Soft broadleaved	99.86%
cutting-site	100%
Road	100%

Chen L, Tian X M, Chai G Q, Zhang, X *; Chen, E. A New CBAM-P-Net Model for Few-Shot Forest Species Classification Using Airborne Hyperspectral Images[J]. Remote Sensing, 2021, 13(7).

Tree Species Classification

Proto-MaxUp Classification Map

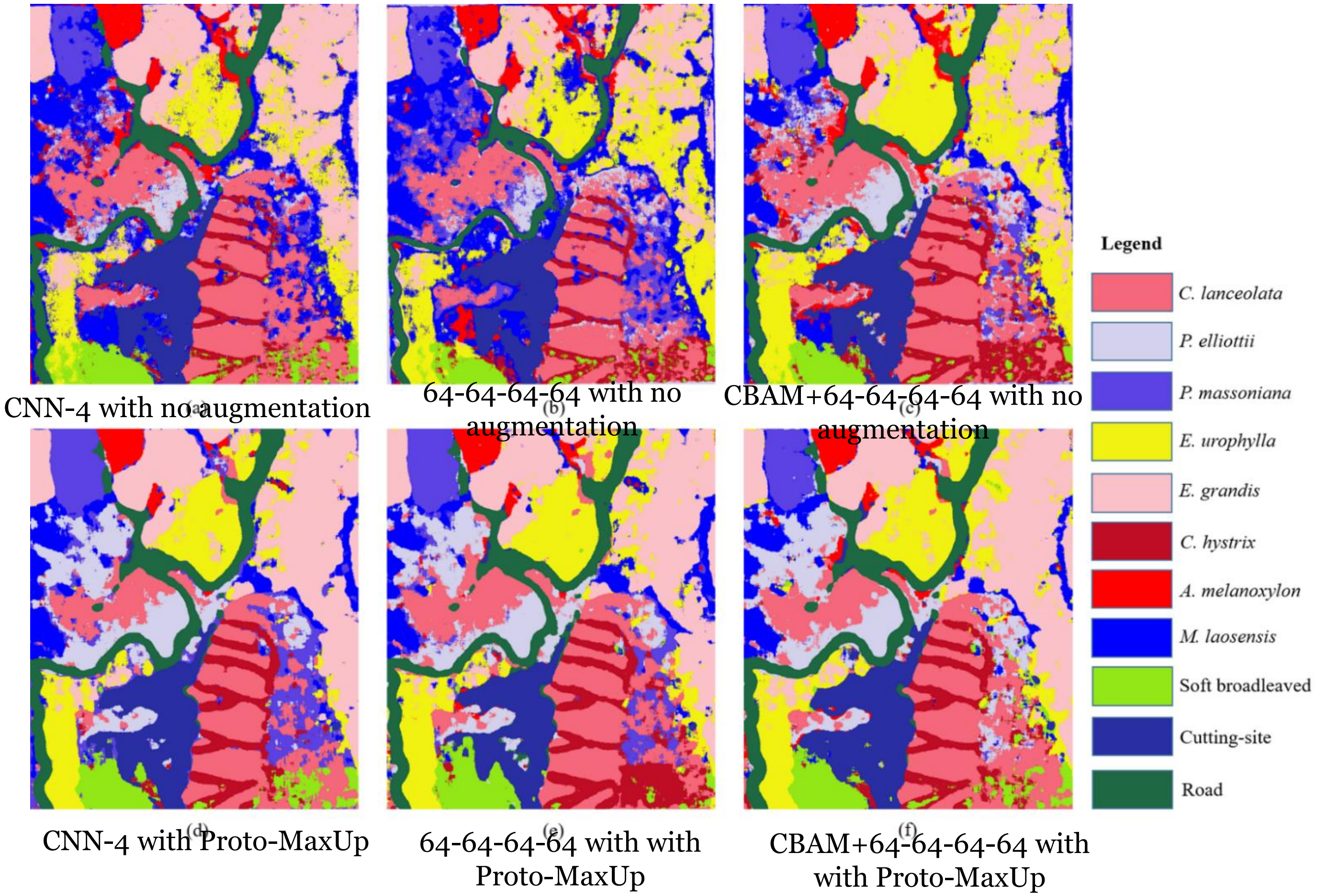

Classification maps of P-Net with different backbones

	23×23
LEA	100%
OA	**98.08%**
Kappa	0.9789
C. lanceolata	98.76%
P. elliottii	98.92%
P. massoniana	99.14%
E. urophylla	97.58%
E. grandis	99.98%
C. hystrix	96.16%
A. melanoxylon	99.58%
M. laosensis	92.56%
Soft broadleaved	98.86%
cutting-site	100%
Road	97.32%

L. Chen, Y. Wei, Z. Yao, E. Chen and X. Zhang, Data Augmentation in Prototypical Networks for Forest Tree Species Classification Using Airborne Hyperspectral Images, IEEE Transactions on Geoscience and Remote Sensing, 2022, 60, 1-16

Individual-Tree Species Identification by ACE R-CNN

- propose an attention mechanism, edge detection and region-based instance segmentation algorithm (ACE R-CNN)
- use UAV LiDAR and RGB images.
- obtain good classification results for **6 major tree species** in southern China.

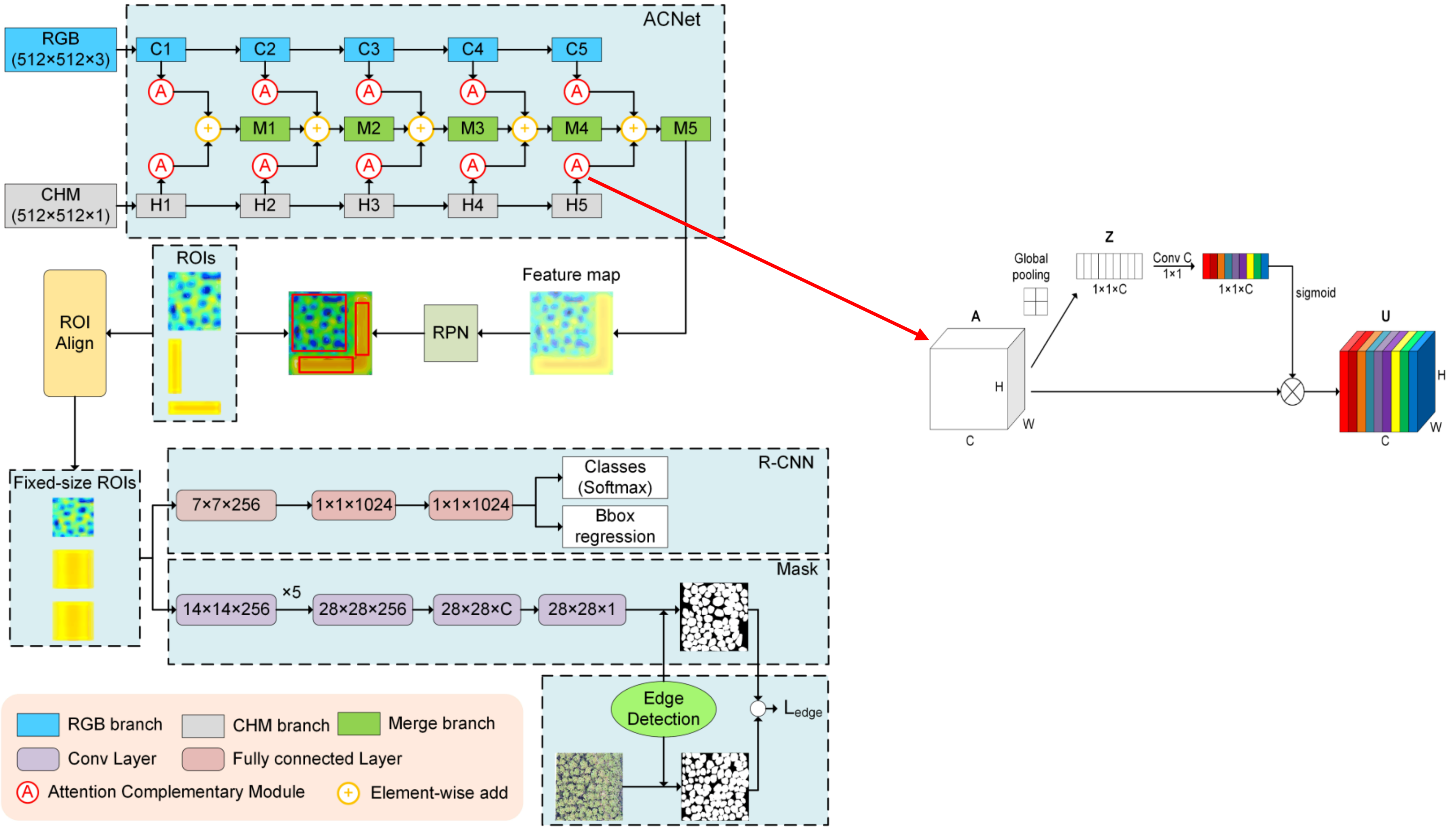

ACE R-CNN Framework

Tree Species Classification

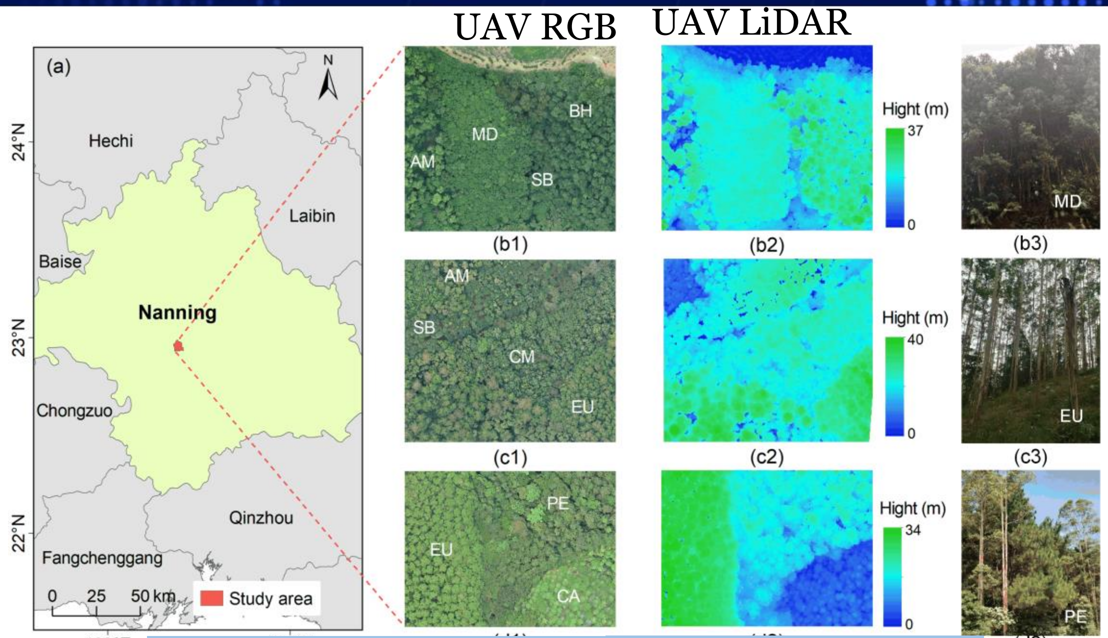

Sample Sets	Tree species	Sample Sets	
		Training Set	Test Set
Experiment area 1	BH	240	172
	MD	291	209
	AM	141	106
	SB	99	80
	Total	771	567
Experiment area 2	AM	146	114
	EU	288	212
	CM	271	192
	SB	235	174
	Total	940	692
Experiment area 3	EU	181	135
	PE	160	116
	CA	147	117
	Total	488	368

Individual-Tree Species Identification Map

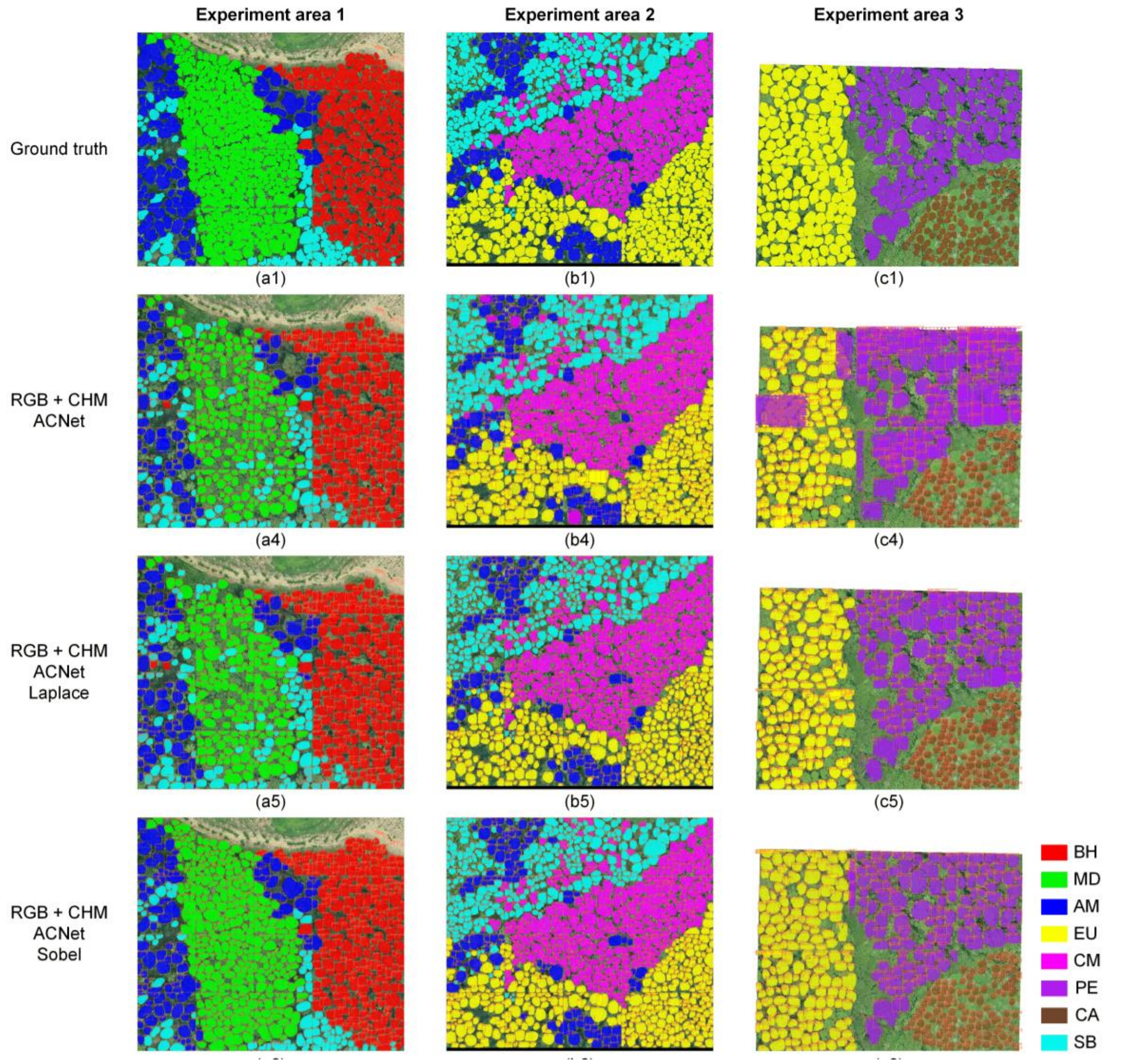

Tree Species Classification from multitemporal satellite images

- Dominant tree species
  - Pine
  - Spruce
  - Birch
  - Oak
  - Larch
- Classification from Sentinel-2 images from three different dates

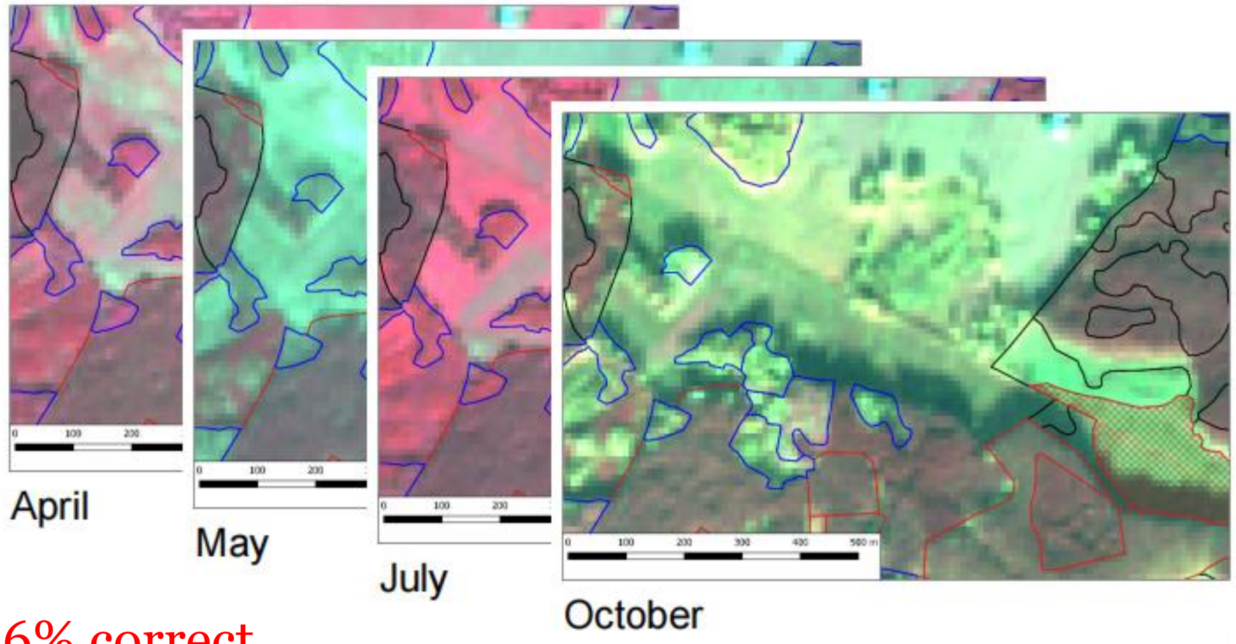

- Result
  - One image, May, 79% correct
    - Two image, May +April, 85% correct
    - Three image, May + April + October, 86% correct

- The July image was very similar to the May image – redundant

Persson, M, Lindberg, E, Reese, H. (2018). Tree Species Classification with Multi-Temporal Sentinel-2 Data Remote Sensing, 10 (11)

Tree Species Classification Combining Images with Bayesian Inference

- Dominant tree species
  - Pine
  - Spruce
  - Birch
  - Oak
  - Larch

- Classification from Sentinel-2 images available from 142 different dates in 2017-2018

- Classification of a combination of images with Bayesian inference

- The method can be implemented operationally for a stream of satellite images

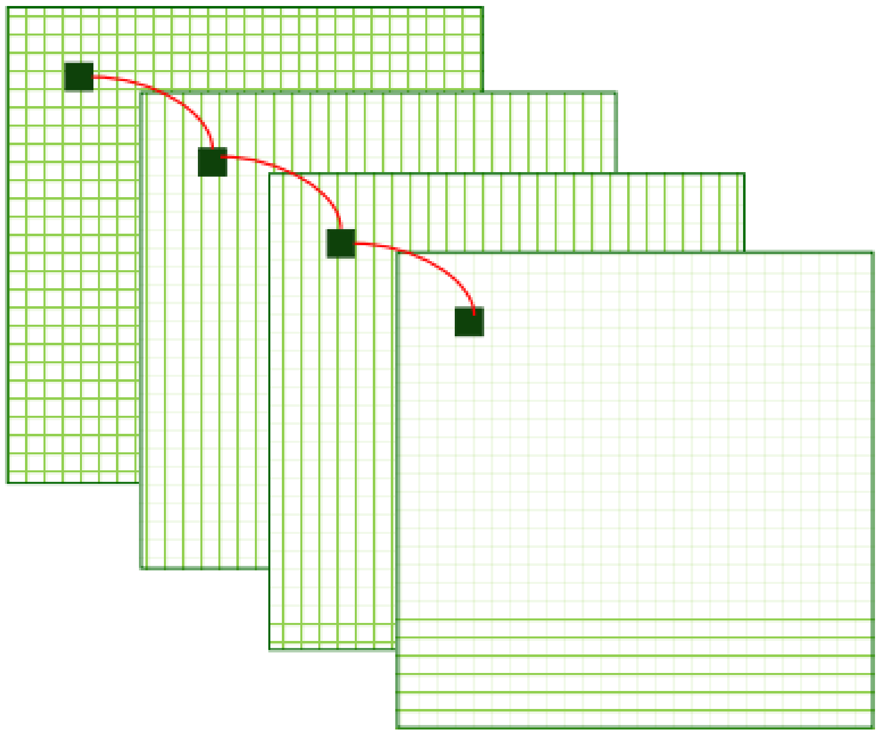

Axelsson, A., Lindberg, E., Reese, H., & Olsson, H. (2021). Tree species classification using Sentinel-2 imagery and Bayesian inference. Int. Journal of Applied Earth Observation and Geoinformation, 100, 102318

Tree Species Classification for Habitat Mapping

- Swedish forests are dominated by two tree species: *Pinus sylvestris* and *Picea abies*
- Other common species are *Betula pubescens* and *Betula pendula*
- More rare tree species include *Populus tremula*, *Alnus incana*, *Salix caprea*, and *Sorbus aucuparia*
- The south of Sweden (southern coniferous-deciduous) has a bigger variety of tree species, including *Alnus glutinosa*, *Quercus robur*, *Fagus sylvatica*, and *Fraxinus excelsior*

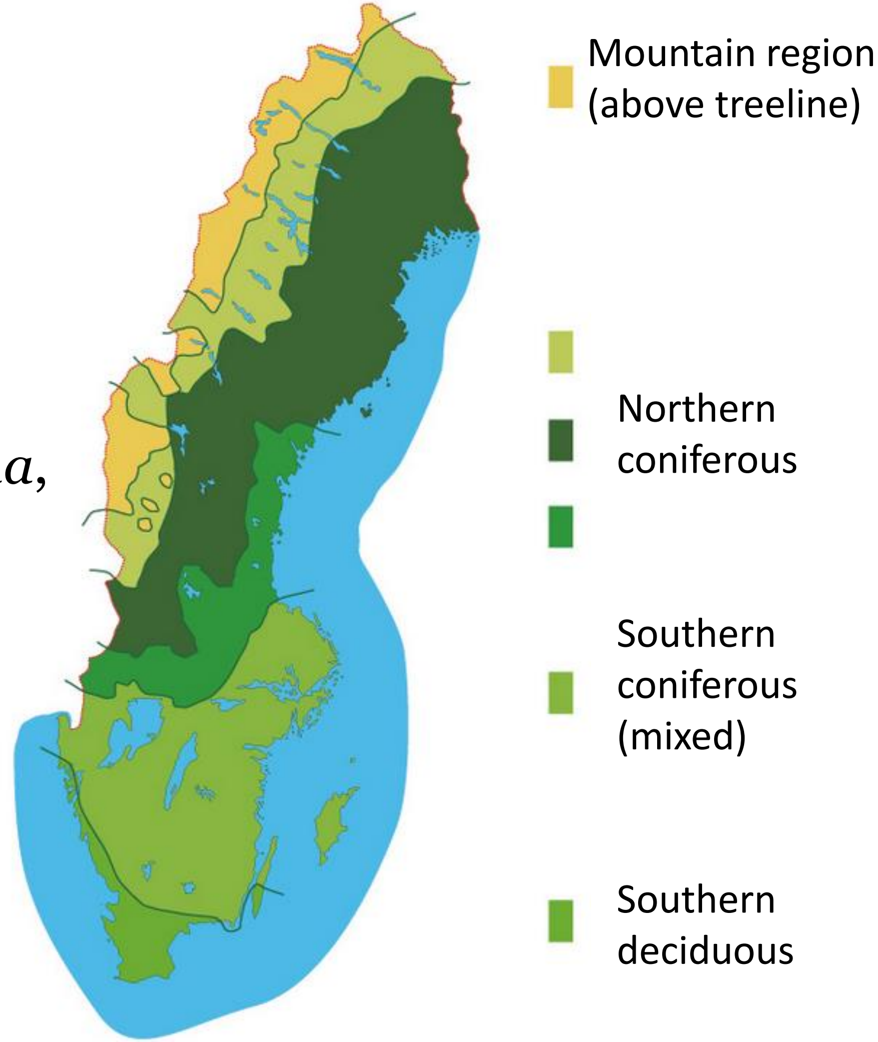

Source: www.skolvision.se @Lars Thang and Boloria AB

Tree Species Classification for Habitat Mapping

- Tree species is relevant for biodiversity since different organisms depend on certain tree species as substrates or for foraging

- The less common tree species are important for some rare species that occur less frequently in the landscape

- Forestry in Sweden has for a long time prioritized the most commercially valuable tree species, making *Pinus Sylvestris* and *Picea Abies* even more common

- Research in Sweden has this far focused on the most common tree species, but habitat mapping would benefit from identification of less common tree species too

Tree Species Classification for Habitat Mapping

- We have currently started a study with the aim to identify less common tree species from multispectral ALS data (Riegl VQ-1560i-DW with wavelengths 1064 nm and 532 nm)
- The study is done in Krycklan in northern Sweden
- Tree crowns will be delineated from ALS data with an automatic method developed by our group
- The tree crowns will be classified based on spectral and geometrical properties similar to a previous study on solitary trees outside of forest

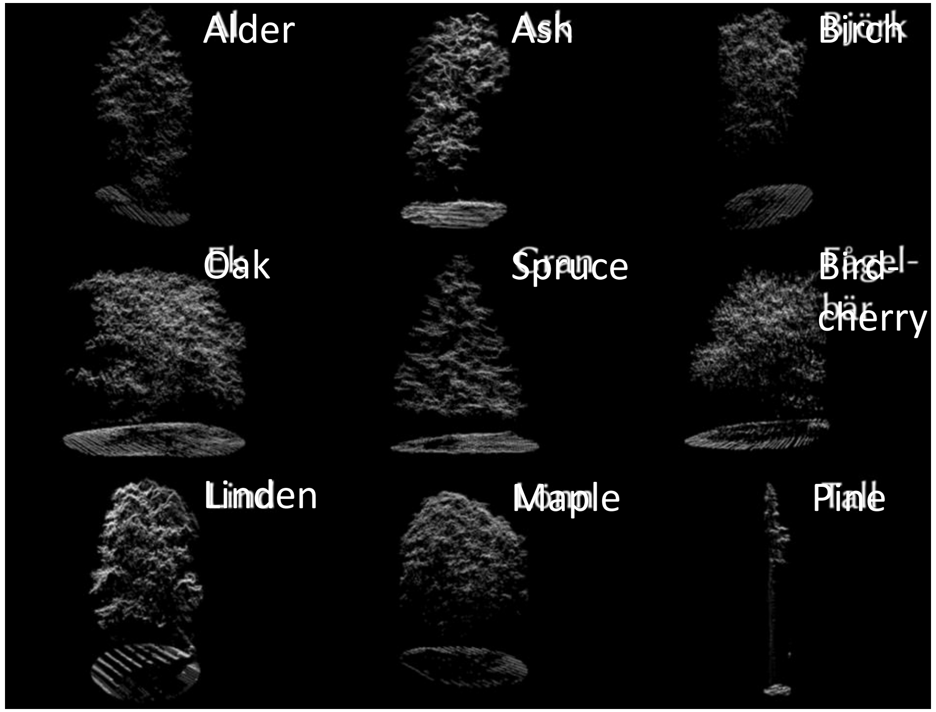

Axelsson, A., Lindberg, E., & Olsson, H. (2018). Exploring Multispectral ALS Data for Tree Species Classification. Remote Sensing, 10, 183

Further research plan

- Tree species classification using WorldView-3 and Sentinel-2 imagery.
- Classification of species of individual trees or area-based classification (raster) using multispectral airborne laser scanning.

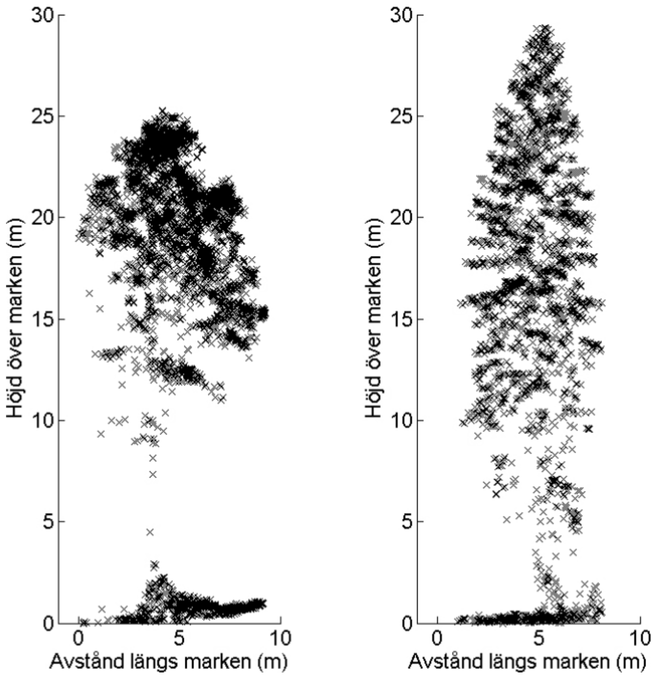

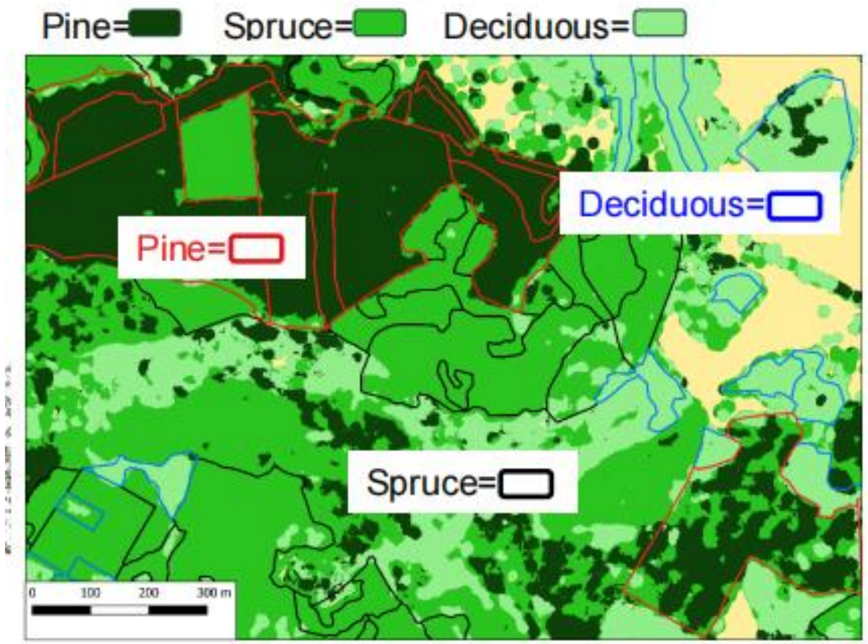

Forest parameter estimation

Individual tree crowns segmentation using UAV oblique photos

- Field data
- UAV oblique photos
- LiDAR data

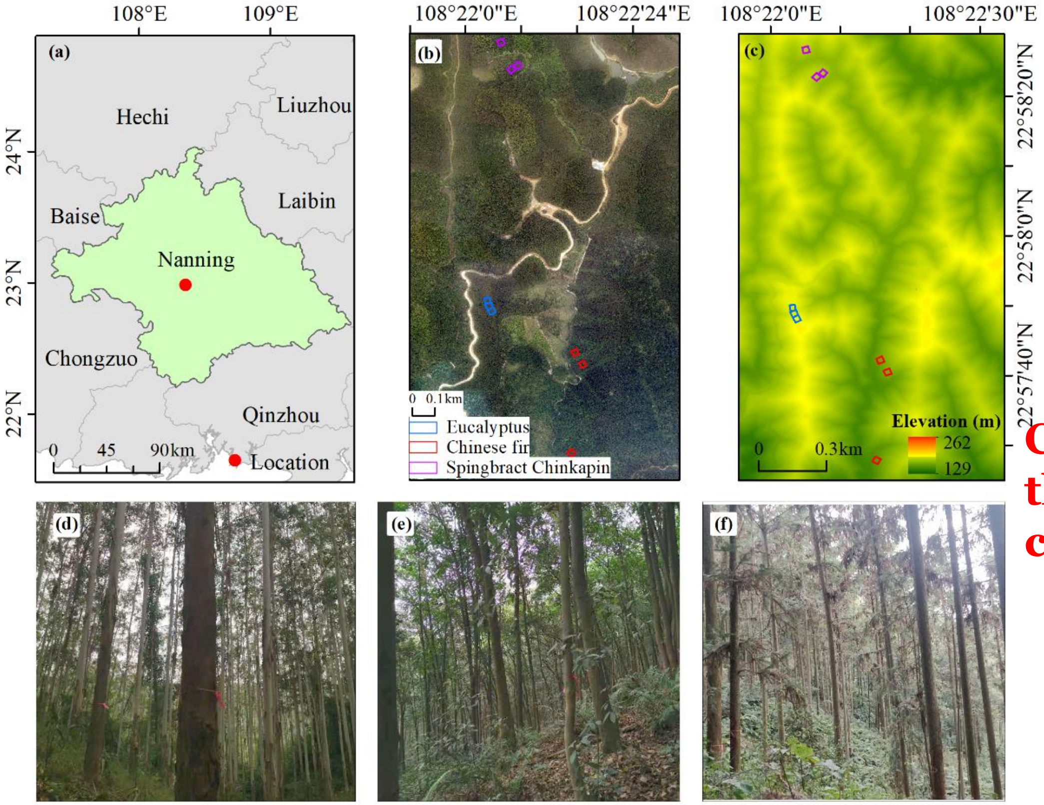

Considering three-dimensional canopy attributes

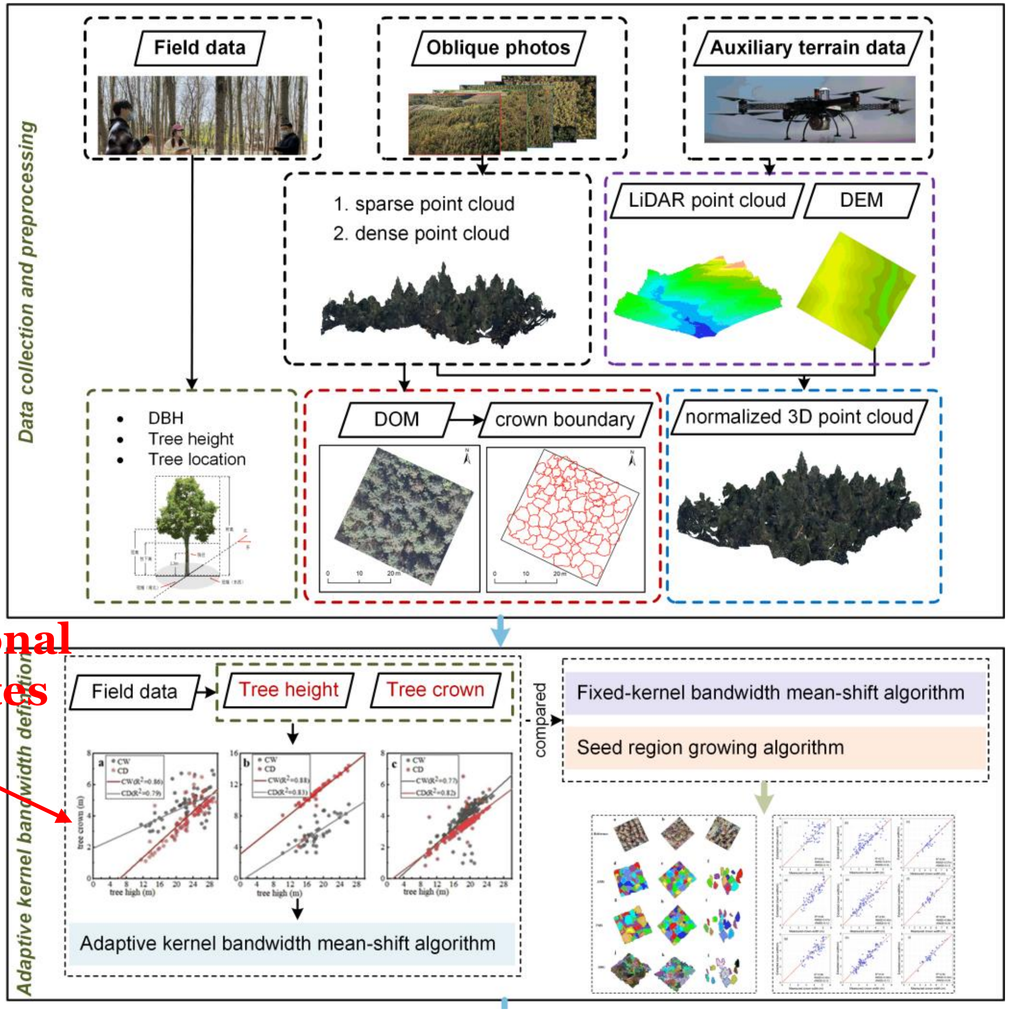

Lei, L.; Yin, T.; Chai, G.; Li, Y.; Wang, Y.; Jia, X.; Zhang, X. A novel algorithm of individual tree crowns segmentation considering three-dimensional canopy attributes using UAV oblique photos. International Journal of Applied Earth Observation and Geoinformation 2022, 112, doi:10.1016/j.jag.2022.102893.

Individual tree crowns segmentation using UAV oblique photos

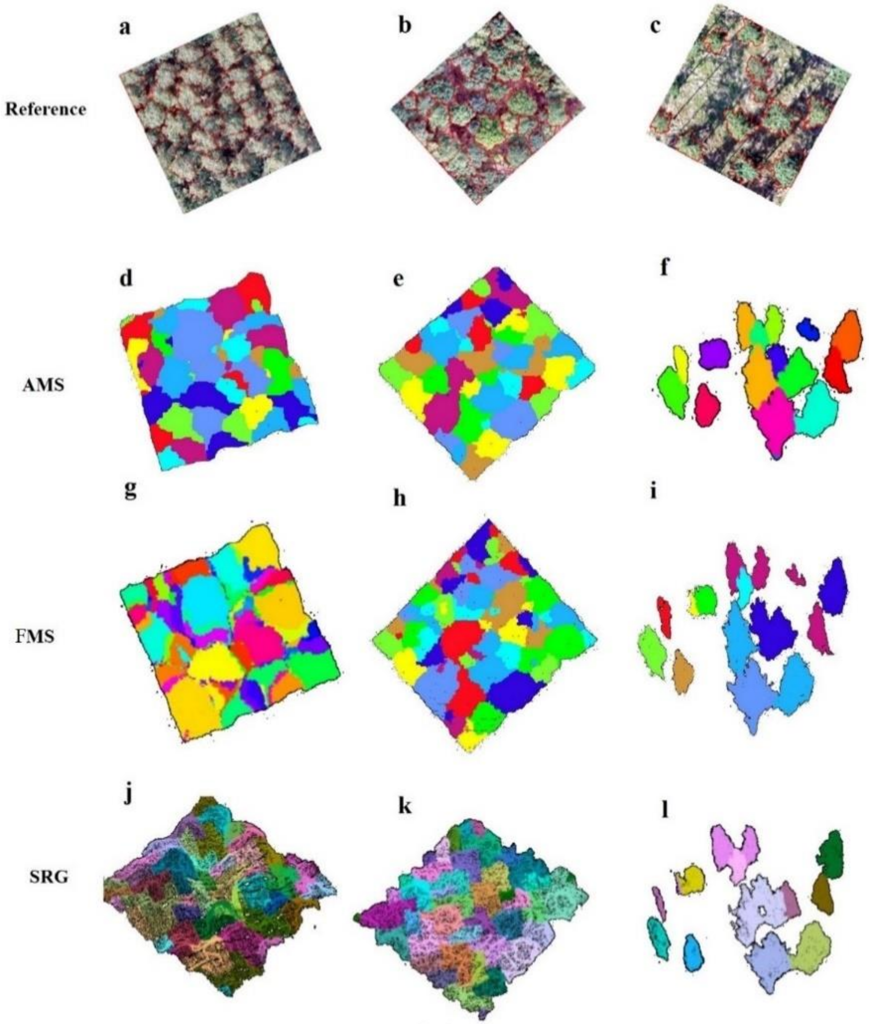

The results of ITCs segmentation (a, d, g, j are Eucalypts, b, e, h, k are Spingbract Chinkapin and c, f, i, l are Chinese fir.)

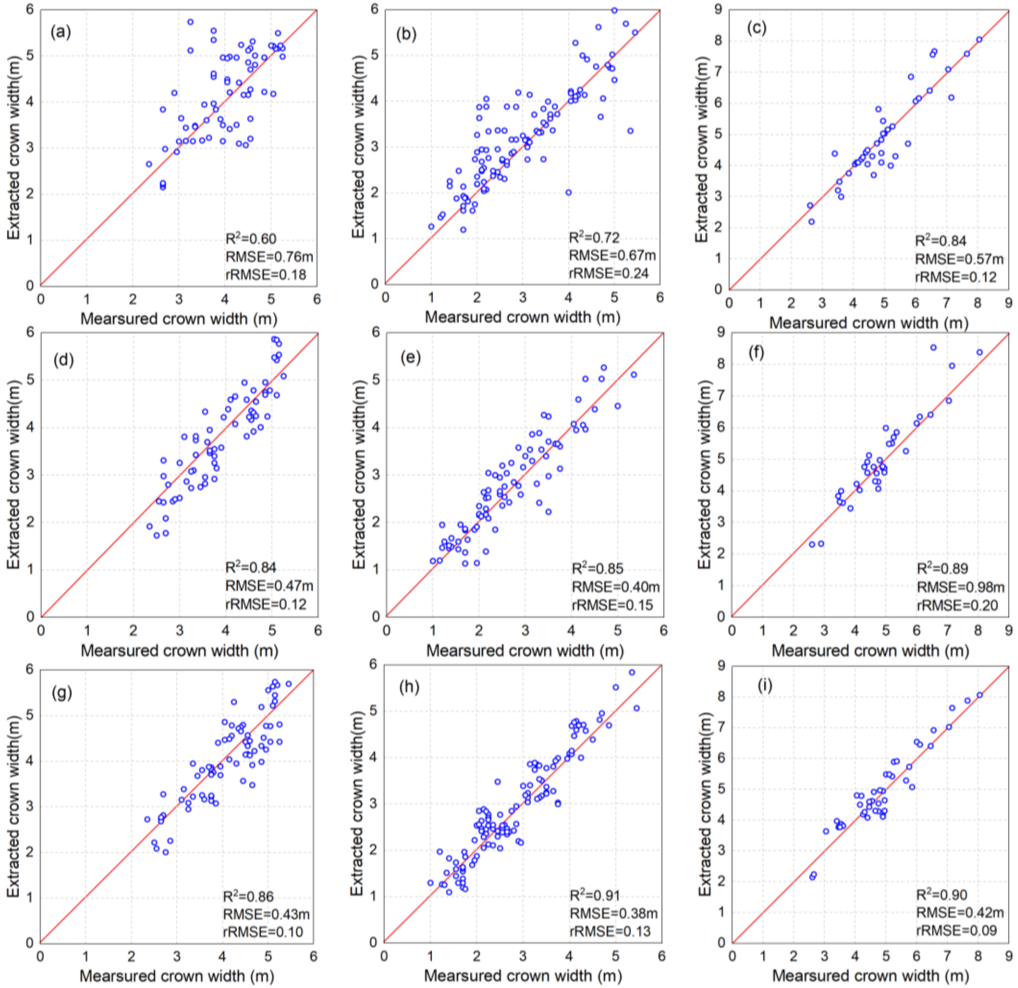

The scatter plots of measured crown width and extracted crown width obtained by the three different methods

- Flexible setting of kernel bandwidth to segment ITC for each tree based on tree height.
- High accuracy can be achieved in both tree top detection and canopy width extraction.
- Appropriate reduction of point cloud density can balance efficiency and accuracy.
- The application of AMS algorithm in LiDAR data is still possible.

Individual tree biomass estimation using UAV oblique photos

Feature variables

- RGB space
- HSI space
- Hight variables
- density variables
- Vegetation index

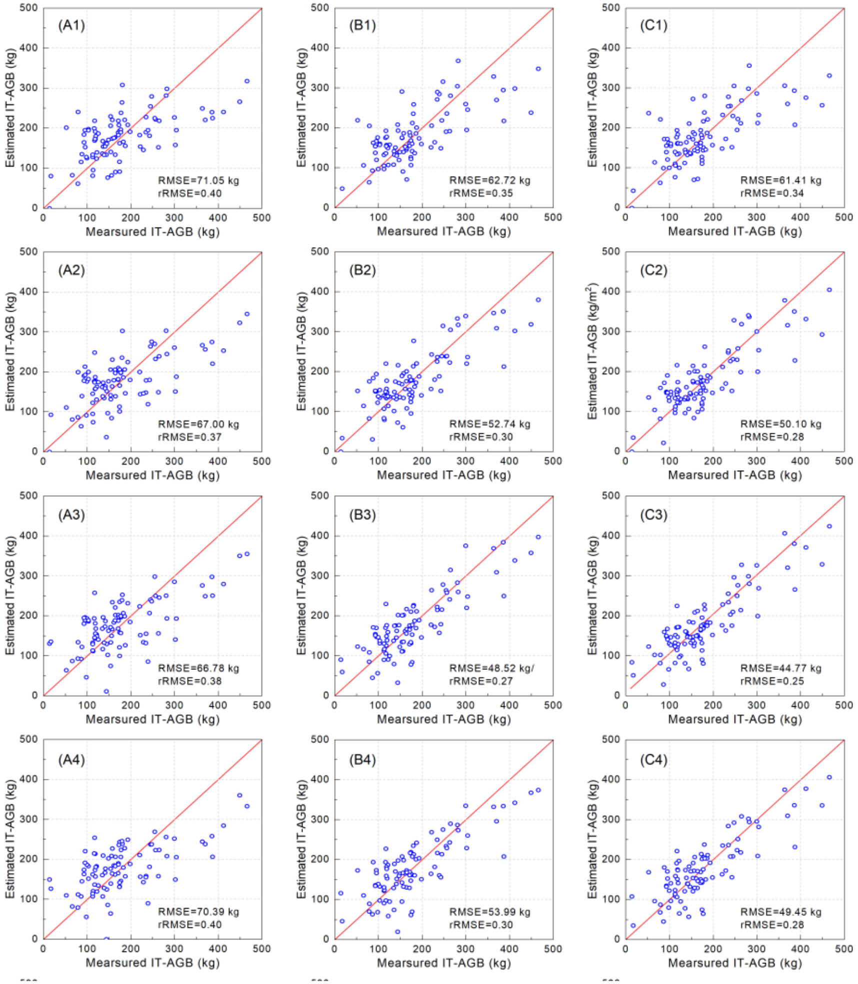

Scatterplots of measured and predicted IT-AGB

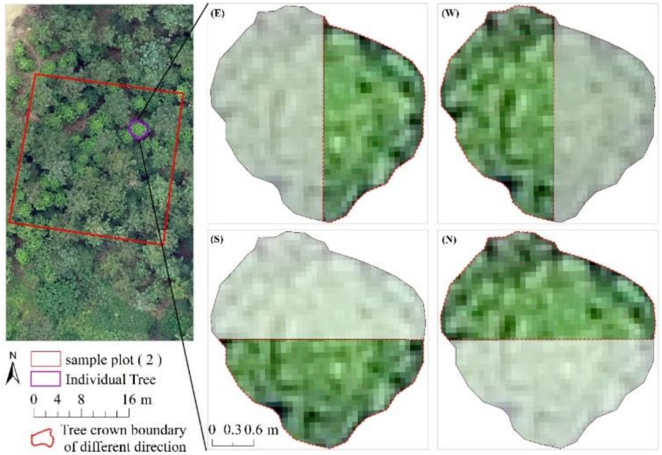

Map of tree canopy division in different directions

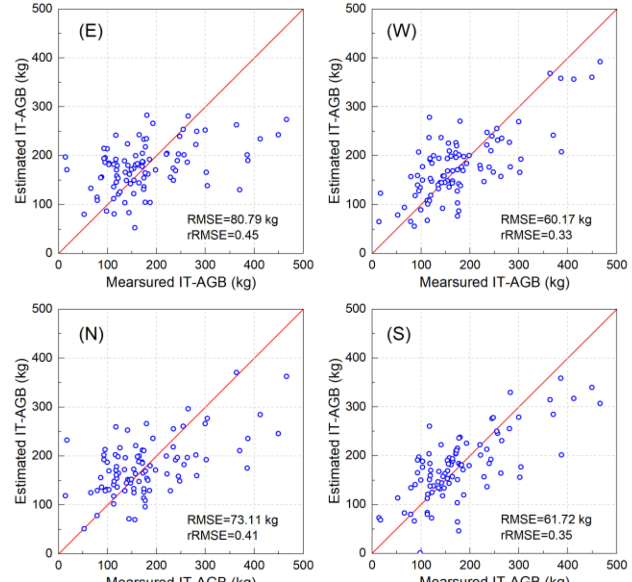

Scatterplots of measured and predicted IT-AGB in different direction.

Lei, L.; Chai, G.; Wang, Y.; Jia, X.; Yin, T.; Zhang, X. Estimating Individual Tree Above-Ground Biomass of Chinese Fir Plantation: Exploring the Combination of Multi-Dimensional Features from UAV Oblique Photos. Remote Sensing 2022, 14, doi:10.3390/rs14030504.

Forest tree height and biomass estimation using multi-source data

- ZY-3 stereo images
- Sentinel-2 multi-spectral image
- ALOS DEM dataset

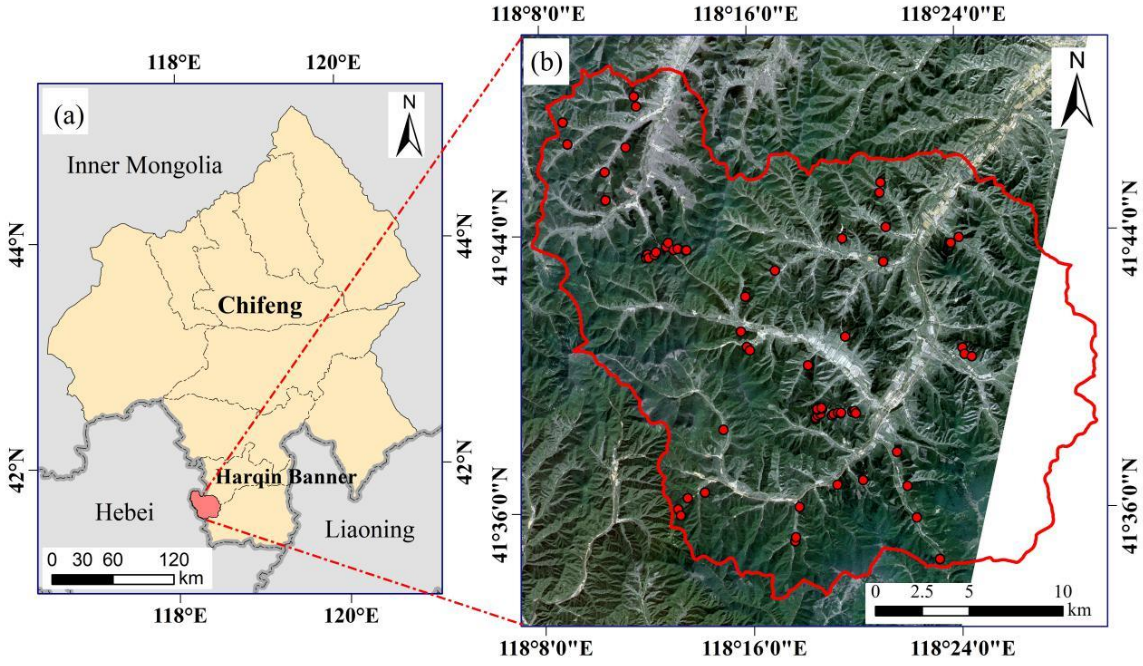

Location of the study area (a) and the distribution of the sample plots (b).

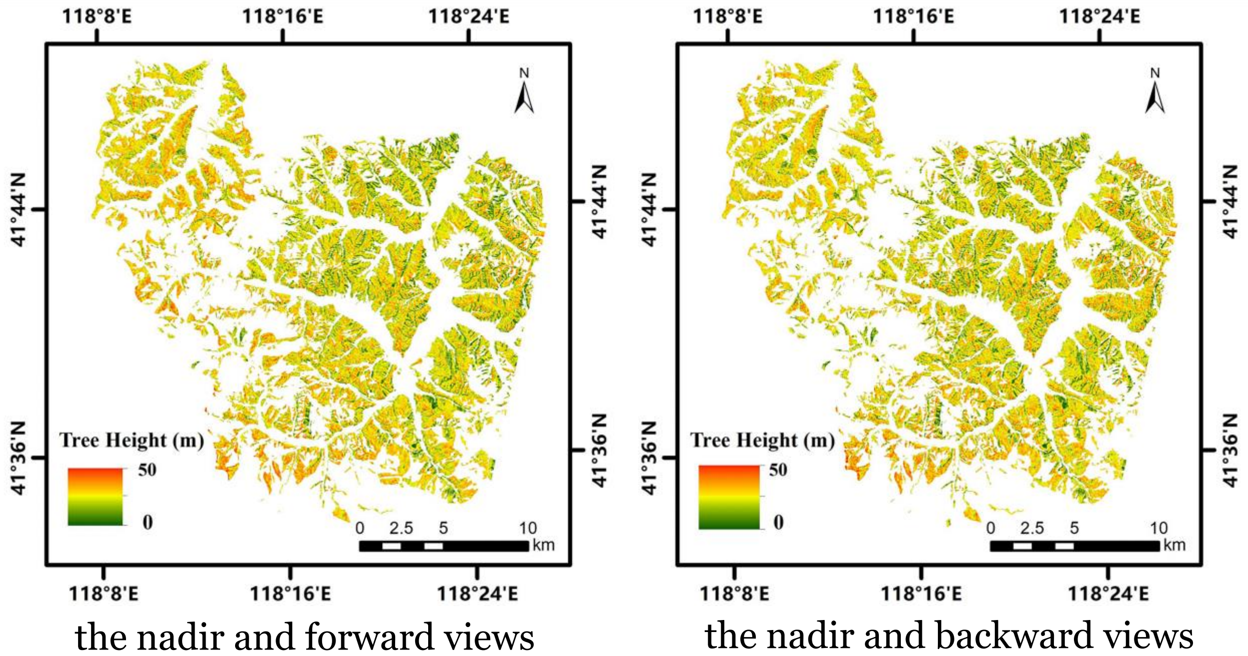

- The nadir and forward views provide better results than the nadir and backward views.
- A high resolution spatially continuous tree height product.

Forest tree height and biomass estimation using multi-source data

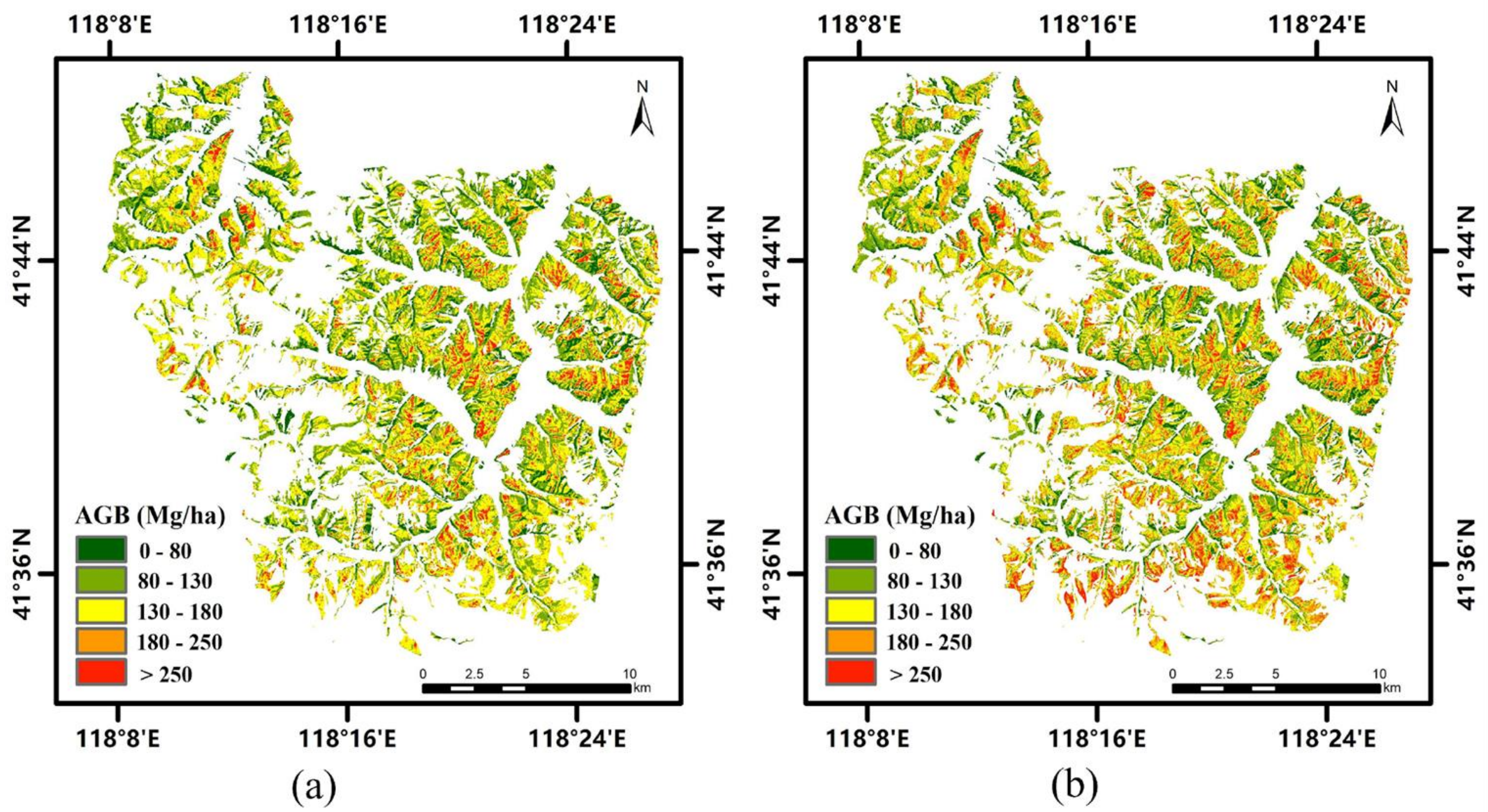

Distribution of the coniferous forests AGB in the Wangyedian Farm (a) without tree height, (b) with tree height.

- Incorporation the tree height information, the coniferous forests AGB estimation can be significantly improved.
- The data saturation problem can be alleviated.

Yueting Wang, Xiaoli Zhang, Zhengqi Guo. Estimation of tree height and aboveground biomass of coniferous forests in North China using stereo ZY-3, multispectral Sentinel-2, and DEM data[J]. Ecological Indicators, 126.

Forest parameter estimation

Biomass estimation using polarimetry

RadarSat-2 (Canadian Space Agency)

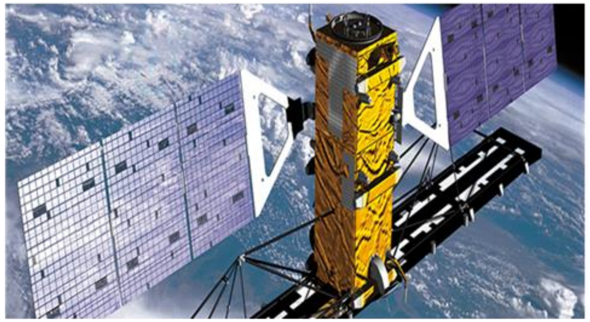

TerraSAR-X (German Aerospace Center (DLR))

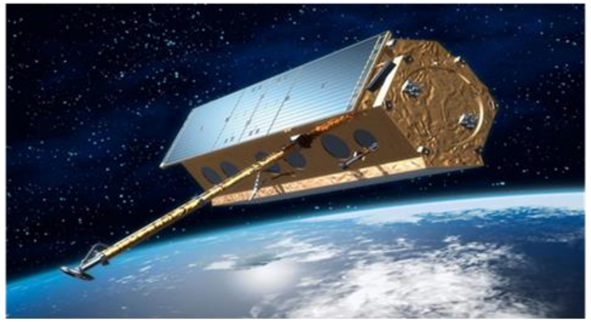

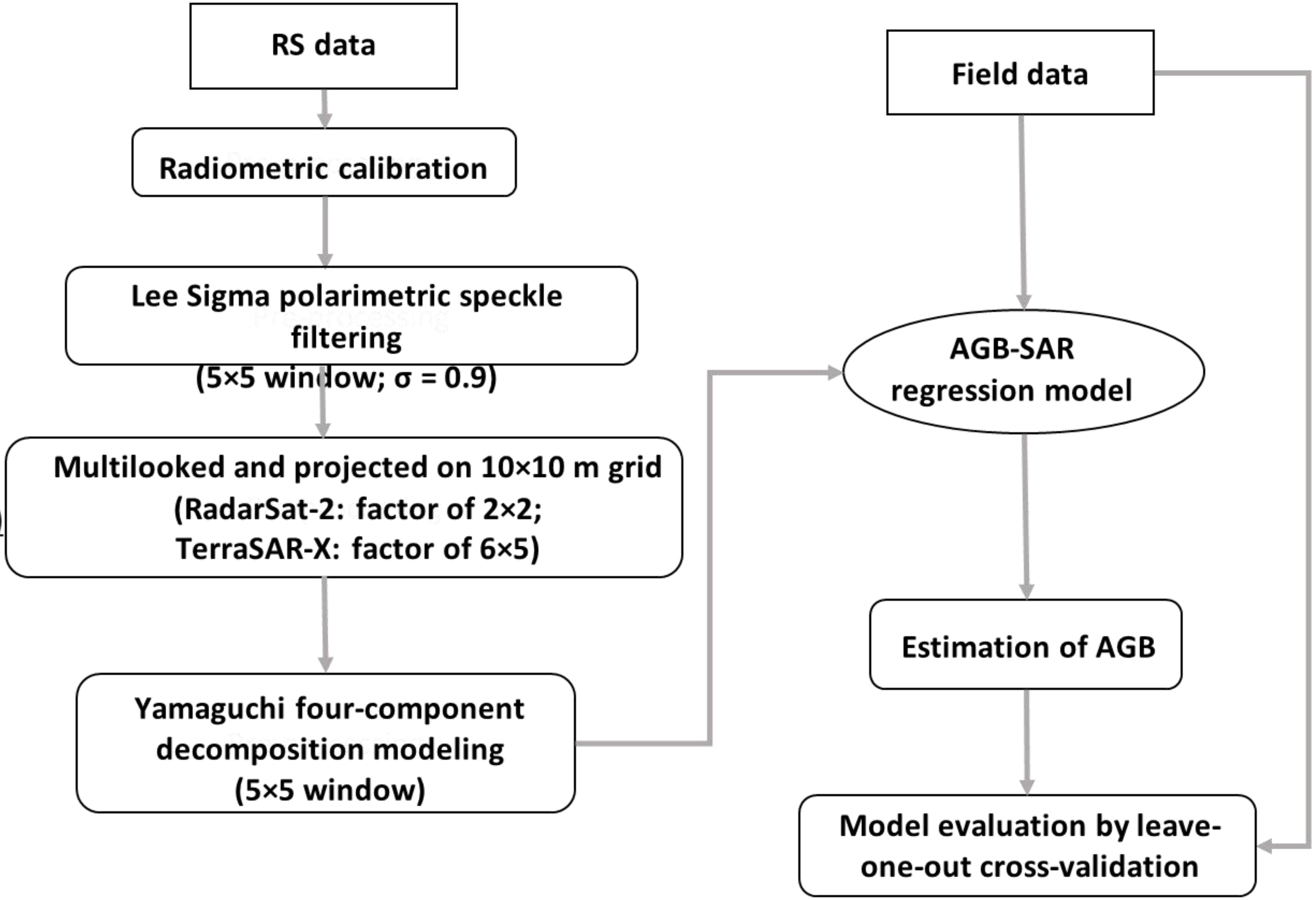

Framework

Presentation by Henrik J. Persson, SLU

Forest parameter estimation

Biomass estimation using polarimetry

(double-bounce) σ^{o}_{dbl} (surface) σ^{o}_{surf} (volume) σ^{o}_{vol} (helix) σ^{o}_{hlx}

Biomass estimation using polarimetry

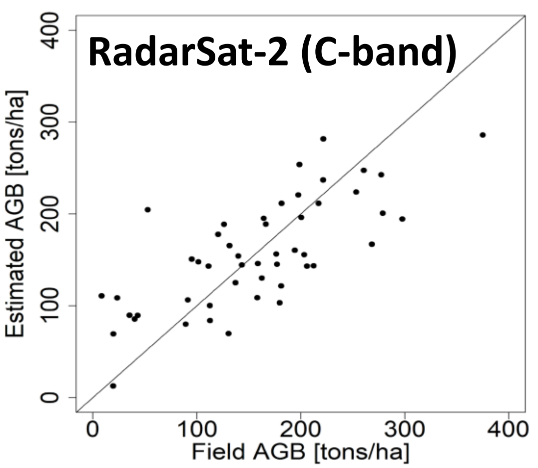

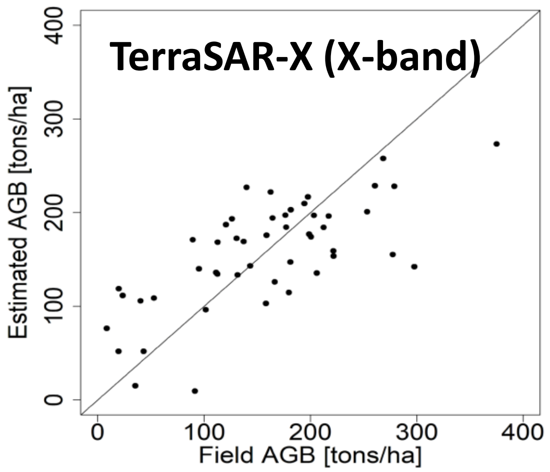

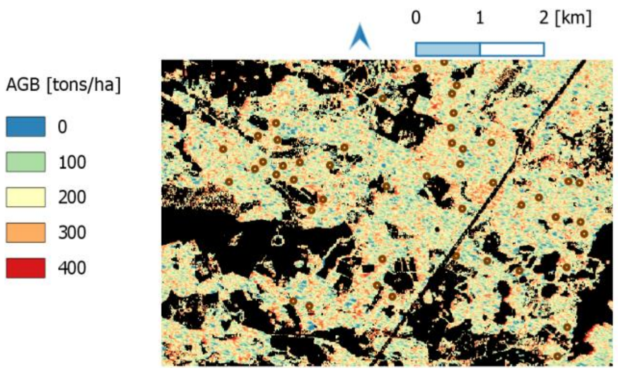

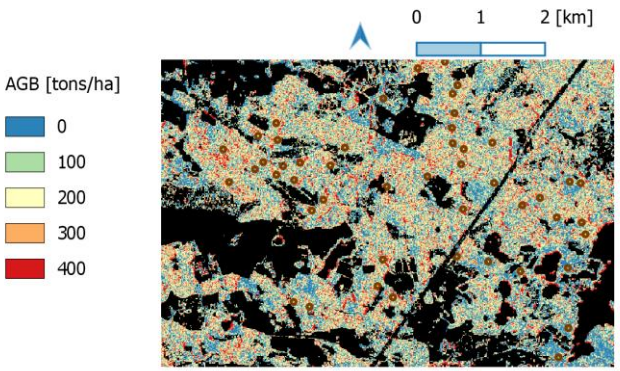

Model statistics:

Sensor	Model	R2	RMSE [tons/ha]	n
RadarSat-2	Estimated	0.52	54.2 (34.6%)	48
TerraSAR-X	Estimated	0.47	56.8 (36.3%)	48
RadarSat-2	LOOCV	-	58.1 (37.1%)	48
TerraSAR-X	LOOCV	-	60.6 (38.6%)	48

- C-band estimates show a linear relationship throughout the full range
- X-band estimates indicate a saturation at about 300 tons/ha
- Difference in the significant explanatory variables in the regression models for C- and X-band may be due to the different penetration capacity of C and X-band
- The resolution of TerraSAR-X was higher compared to RadarSat-2, which might result in more homogenous scattering within each SAR resolution cell resulting in higher contribution of surface and double bounce scattering
- Yamaguchi polarimetric decomposition technique is a useful approach when estimating biomass in coniferous dominated hemi-boreal forest
- Potential of using only SAR polarimetry is lesser compared to approaches where height information are available (e.g., single-pass interferometry from TanDEM-X)

Treatment Detection Using InSAR Time Series

TanDEM-X (German Aerospace Center (DLR))

RS data

Time series of 24 VV polarization scenes.
Aug 2011 - June 2014

Processed to obtain interferometric height using 2 m x 2 m DTM, final phase height products 10 m × 10 m in ground resolution.

Pixel level penetration depth correction: (ha: height of ambiguity, γ: coherence)

$$\Delta h = -\frac{|h_a|}{2\pi}\arctan(\sqrt{|\gamma|^{-2} - 1}), \qquad (1)$$

Field data

34 plots, 40m in radius. located inside homogenous stands.

Treatment records in forest management plan used to classify plots into 25 untreated, 5 thinned, and 4 clear-cut.

I. Huuva, H.J. Persson, J. Wallerman, and J.E.S. Fransson, "Detectability of Silvicultural Treatments in Time Series of Penetration Depth Corrected TanDEM-X Phase Heights," In *Proceedings of IGARSS 2022,* Kuala Lumpur, Malaysia

Treatment Detection Using InSAR Time Series

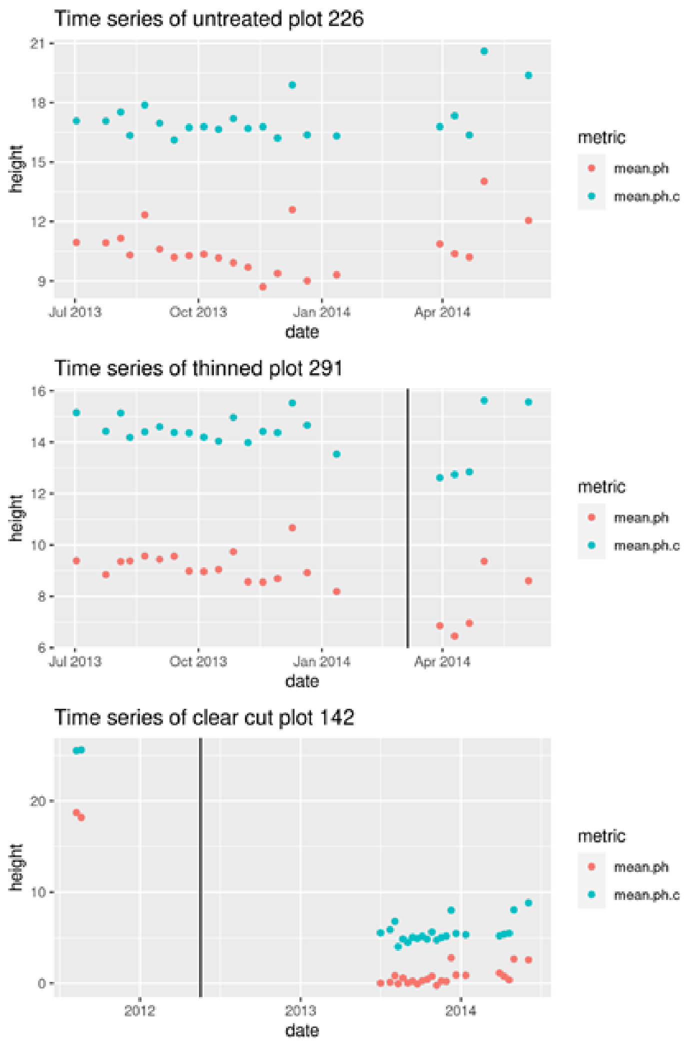

Phase height time series

Top: Untreated plot, more or less constant phase height, albeit with significant variance in height from date to date.

Middle: Thinned plot, decrease in phase heights after treatment, But still some high measurements after treatment.

Bottom: Clear cut plot, Large (20 m) decrease in phase heights after treatment.

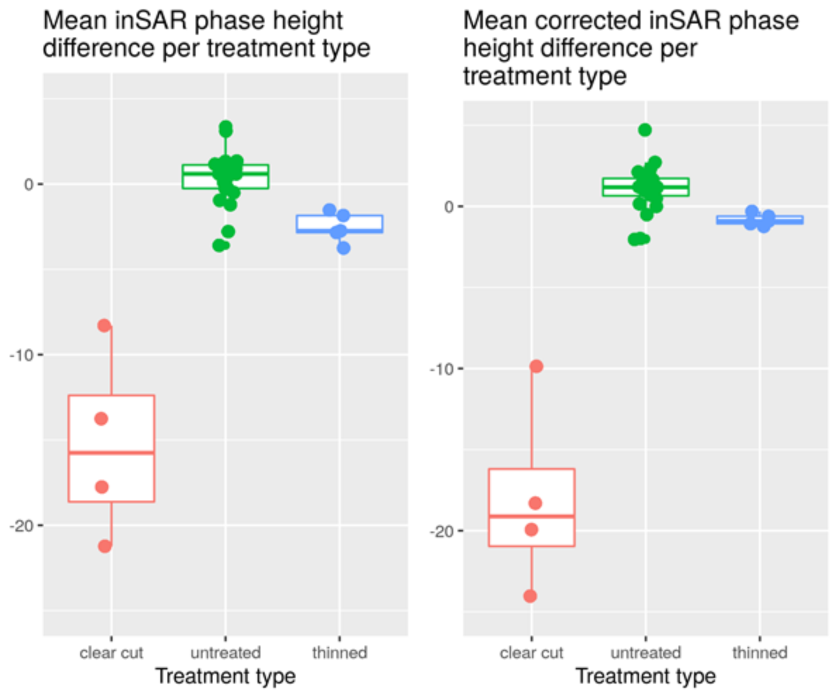

Results

Phase heights decreases from clear cuts clearly distinguishable from untreated and thinned plots.

Thinned plots show decrease in phase heights, but so do some untreated plots, making thinned plots hard to identify.

Table 1. Mean phase height change after treatment (m) with 'Untreated' included for baseline.

Metric	Untreated	Thinned	Clear-cut
Phase height	0.404896	-2.53911	-15.2584
Corrected phase height	1.233816	-0.8281	-18.0332

Further research plan

- Methods for mapping forest and forest change using satellite borne radar (e.g., Sentinel-1 SAR)

  – Developing new algorithms and tools to meet the new requirements in accuracy and precision to map forest state and change both nationally and internationally.

  – Using satellite borne radar, with support of national laser scanning data.

- Detection and mapping of storm damaged forest using spaceborne synthetic aperture SAR

  –Developing methodology and algorithms

  –Perform a scientific evaluation of SAR data from two or more satellite sensors for detecting and mapping changes in boreal forests.

Presentation by Henrik, SLU

Forest Insect Damage Detection

Monitoring of Pine Wilt Disease

- Classification of pine wilt disease at different infection stages

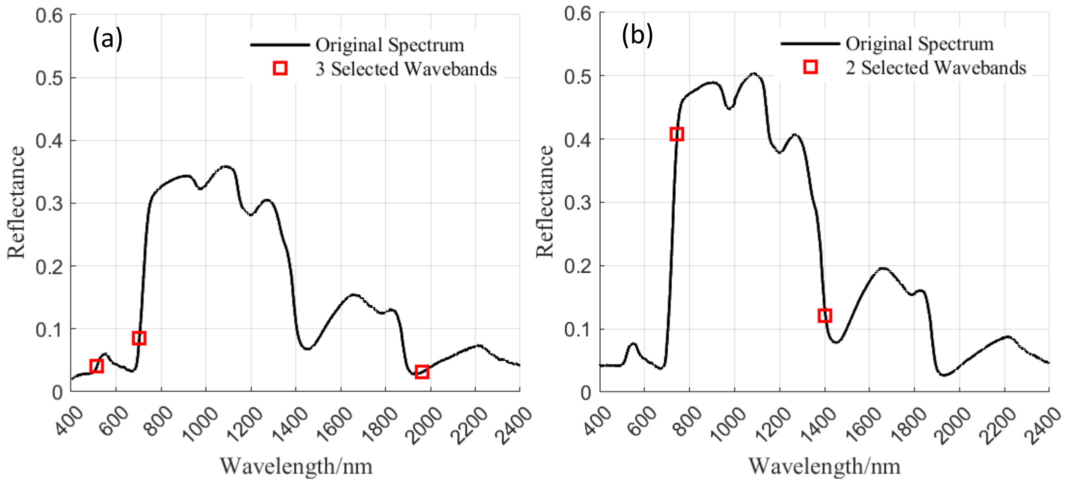

Figure. The sensitive bands of Japanese pine (a), Korean pine (b) selected by CARS-SPA.

Modeling method	Band select Algorithm	Modeling algorithm	Number of bands selected	Validation set				
				H	E	M	L	Total
Japanese pine	All bands	SVM-Linear	2001	0.82	0.58	1.00	0.89	0.78
		SVM-Polynomial	2001	0.73	0.83	1.00	0.56	0.75
		SVM- RBF	2001	0.27	0.42	1.00	0.78	0.53
	SPA	LDA	6	0.73	0.63	0.85	0.83	0.75
	CARS	LDA	15	0.70	0.63	0.79	0.79	0.72
	CARS-SPA	LDA	3	0.85	0.58	0.83	0.90	0.77
Korean pine	All bands	SVM-Linear	2001	0.91	0.75	0.40	1.00	0.79
		SVM-Polynomial	2001	0.27	0.88	0.40	1.00	0.57
		SVM- RBF	2001	0.82	0.63	0.00	1.00	0.64
	SPA	LDA	12	0.85	0.60	0.73	0.71	0.74
	CARS	LDA	14	0.75	0.67	0.76	0.88	0.74
	CARS-SPA	LDA	2	0.86	0.65	0.82	0.87	0.78

Table. Classification accuracy of Japanese pine and Korean pine samples using different selected bands and all bands. H, E, M, L represent the classes of healthy, early-, middle-, and late-stage infected samples.

Niwen Li, Langning Huo, Xiaoli Zhang. Classification of pine wilt disease at different infection stages by diagnostic hyperspectral bands[J]. Ecological Indicators, 2022, 142: 109198.

Monitoring of Pine Wilt Disease

➢ Identifying pine wilt disease using hyperspectral drone images

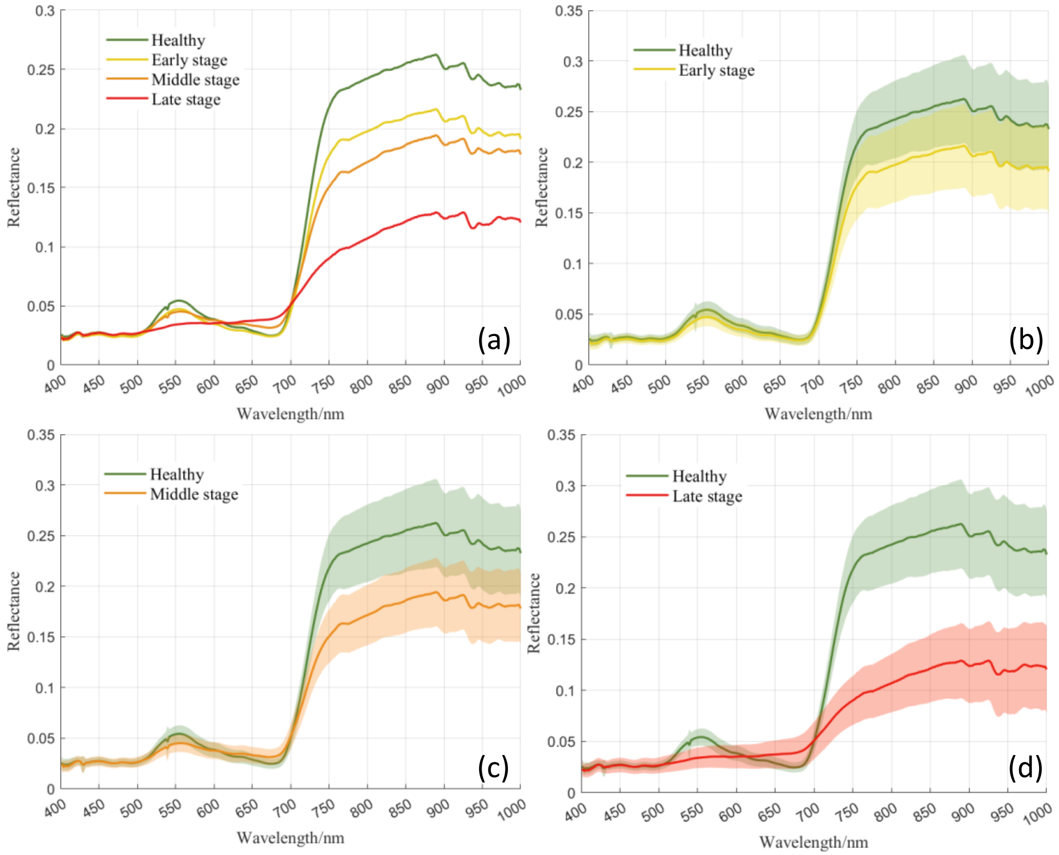

Figure. Mean spectral signature of tree crowns indifferent health status (a) and comparison between healthy and infected trees on the mean and standard deviation (std) of spectral signatures (b - d).

Classification accuracy for different stages

Classified stages	Sensitive wavelength used for classification	Producer accuracy				Overall accuracy
		Healthy	Early stage	Middle stage	Late stage	
All stages	All 270 Bands	0.65	0.35	0.76	0.94	0.68
All stages	758 nm, 553 nm, 889 nm, 524 nm	0.71	0.76	0.35	0.71	0.63
Early stage / healthy	720 nm,680 nm	0.71	0.47	–	–	0.59
Middle stage / healthy	642 nm, 535 nm, 709 nm, 402 nm	1.00	–	0.59	–	0.79
Late stage / healthy	535 nm, 433 nm, 593 nm, 426 nm, 758 nm, 954 nm, 417 nm	0.94	–	–	1.00	0.97

Niwen Li, Xiaoli Zhang, Langning Huo. Identifying nematode-induced wilt using hyperspectral drone images and assessing the potential of early detection. IGARSS 2022.

Forest Insect Damage Detection

Monitoring of European Spruce Bark Beetles

➢ Early detection and large area mapping using Sentinel-2 images

- A new vegetation index (NDRS) was proposed to map the bark beetle damages.
- Spectral differences were observed before attacks

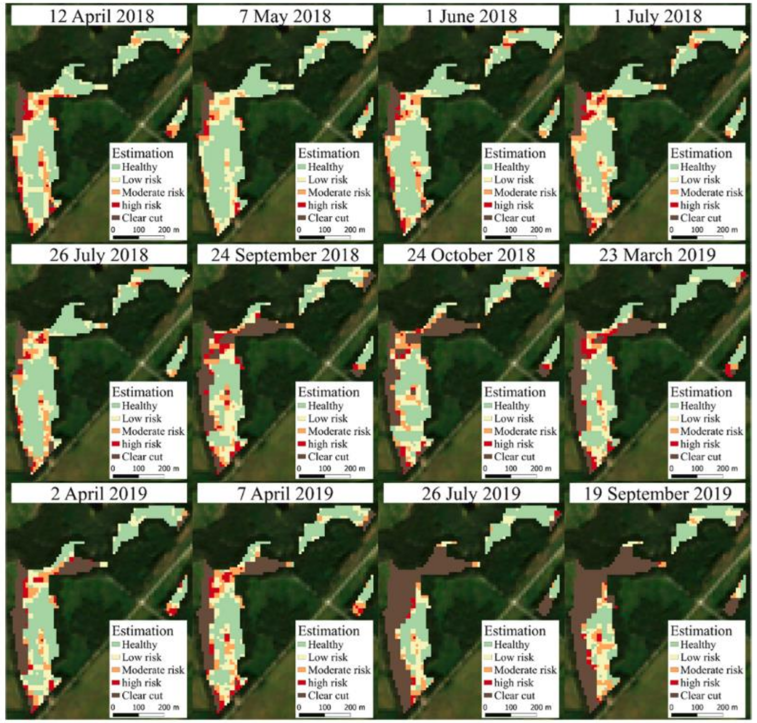

Fig. A5. A case study showing estimated attacks in a time-series and the spatial spread pattern of bark beetle infestations.

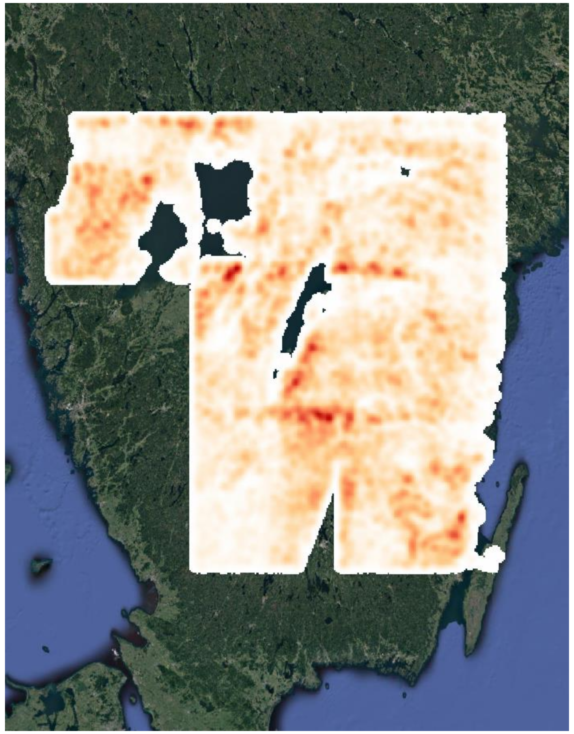

Huo L, Persson H, Lindberg E., 2021. Early detection of forest stress from European spruce bark beetle attack, and a new vegetation index: Normalized Distance Red & SWIR (NDRS). Remote Sensing of Environment, 255, 112240.

Monitoring of European Spruce Bark Beetles

➢ Early detection using drone images

- Multispectral drone images were used with the same wavelengths of Sentinel-2.
- How early did the infested trees show abnormal spectra was investigated.
- The continuous changes of the detectability during green-attacks was quantified.

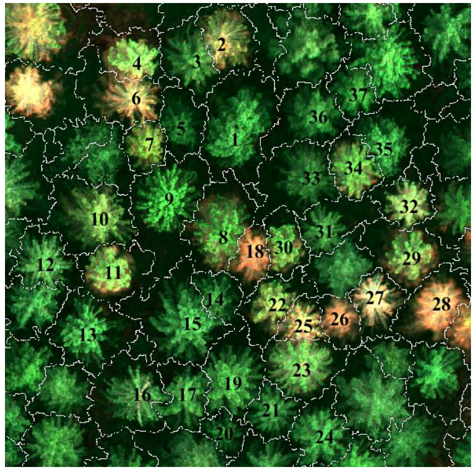

Segmentation of individual tree crowns in a drone image

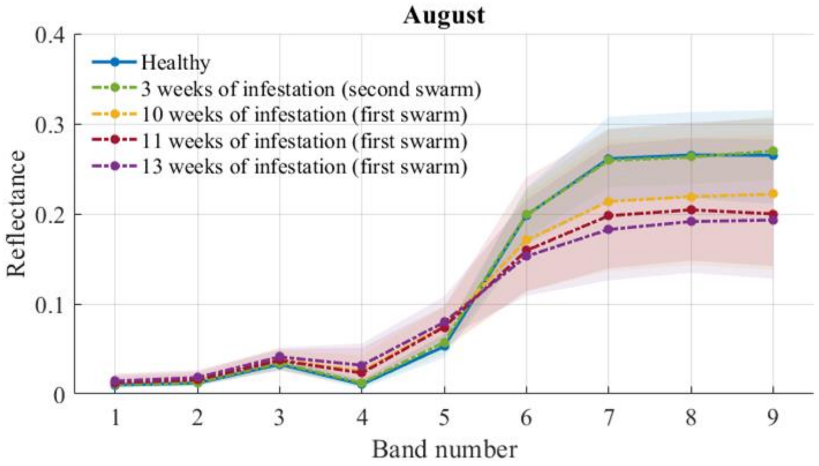

Spectral signatures of tree groups infested for different duration

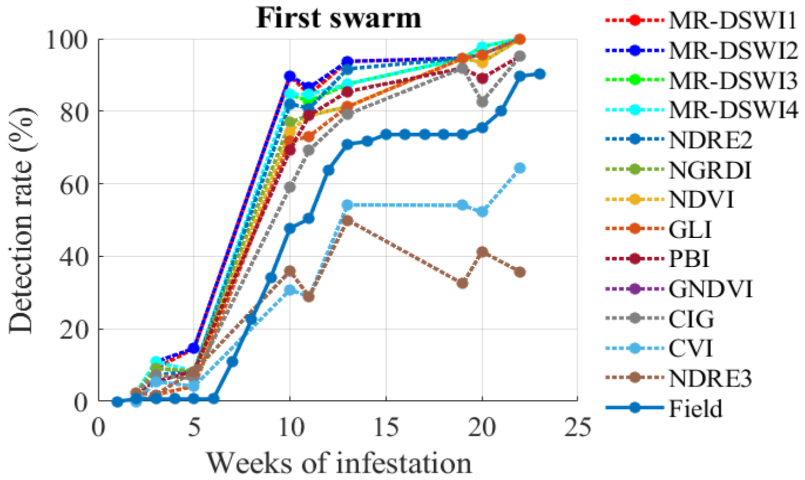

Detectability increased rapidly during 5 – 10 weeks of infestation

Forest Insect Damage Detection

Monitoring of European Spruce Bark Beetles

➢ Is green-attacks detectable using satellite images?

- Sentinel-2

The number of attacked trees limited the time of detection

- ◆ Attacks with >20 trees showed abnormal spectral before attacks.
- ◆ Attacks with >10 trees can be identified in August.
- ◆ Attacks with 5-10 trees can be identified in September.
- ◆ Attacks with <5 trees cannot be identified.

- WorldView-3 SWIR

No significant differences in June

- ◆ Too early in the infestation stage
- ◆ Shadow effects

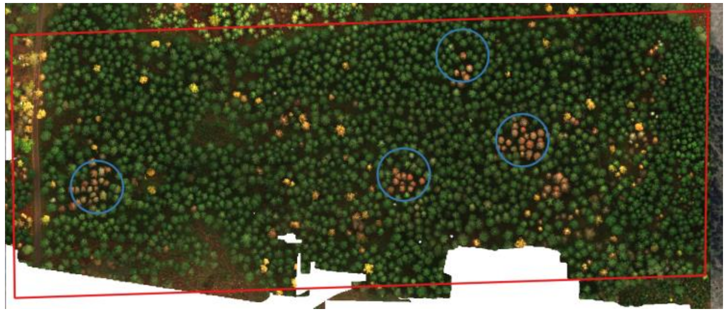

A drone image

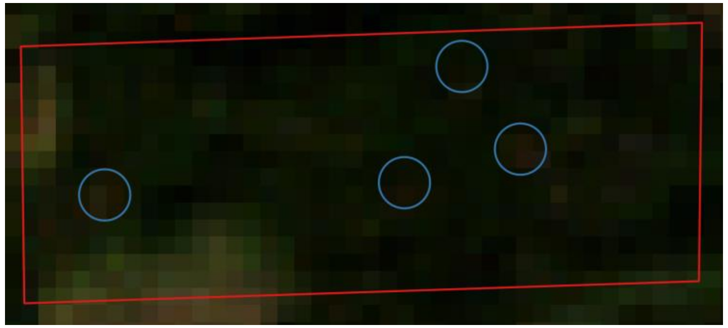

A Sentinel-2 image

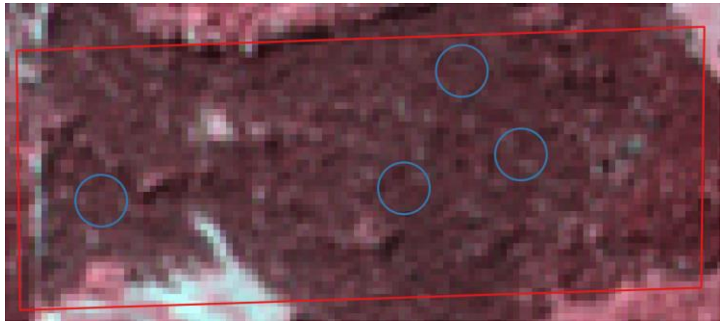

A WorldView-3 SWIR image

Further research plan

- Explore the potential of **hyperspectral drone images** on the early detection of infestations.
- Explore the **environmental factors** of bark beetle damage levels.
- Implement and improve the method of **large-area forest damage mapping** using satellite images.

Two years of collaborative research

- Co-supervising 1 PhD student
- One joint research paper (accepted for publication in Ecological Indicators), one manuscript, and one published conference paper (IGARSS 2022)
- Online Academic Meeting
- Data sharing

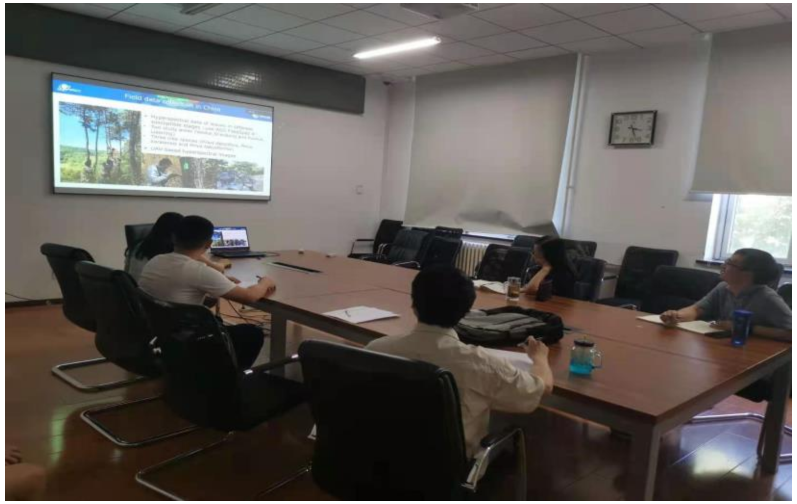

Cooperation plan

- Co-supervising 1~2 PhD students.
- Co-publishing 2~3 research papers.
- Co-organizing an international summer school on forest parameters and deforestation mapping using remote sensing data.

Thank You!

Beijing Forestry University

PI China: Prof. Xiaoli Zhang
Chinese investigators:
Dr. Ning Zhang
Dr. Yueting Wang
Dr. Niwen Li
Dr. Guoqi Chai
Dr. Lingting Lei
Dr. Long Chen
Dr. Xiang Jia
Dr. Zongqi Yao

Swedish University of Agricultural Sciences

PI Europe: Dr. Johan Fransson
European investigators:
Dr. Langning Huo
Dr. Henrik Persson
Dr. Eva Lindberg
Dr. Ivan Huuva